A captorhinid-dominated assemblage from the palaeoequatorial Permian of Menorca (Balearic Islands, western Mediterranean)

Rafel Matamales-Andreu[1,2]*, Francesc Xavier Roig-Munar[3], Oriol Oms[4], Àngel Galobart[1,5] & Josep Fortuny[1]

[1] Institut Català de Paleontologia Miquel Crusafont, Universitat Autònoma de Barcelona, Edifici ICTA-ICP, c/ Columnes s/n, Campus de la UAB, 08193 Cerdanyola del Vallès, Barcelona, Spain.

[2] Museu Balear de Ciències Naturals, ctra. Palma-Port de Sóller km 30, 07100 Sóller, Mallorca, Illes Balears, Spain.

[3] C/ Carritxaret 18-6, 07749 es Migjorn Gran, Menorca, Illes Balears, Spain.

[4] Departament de Geologia, Universitat Autònoma de Barcelona, avda. de l'Eix Central s/n, Campus de la UAB, 08193 Cerdanyola del Vallès, Barcelona, Spain.

[5] Museu de la Conca Dellà, c/ del Museu 4, 25650 Isona i Conca Dellà, Lleida, Spain.

*Corresponding author. E-mail address: rafel.matamales@icp.cat.

Abstract

Moradisaurine captorhinid eureptiles were a successful group of high-fibre herbivores that lived in the arid low latitudes of Pangaea during the Permian. Here we describe a palaeoassemblage from the Permian of Menorca (Balearic Islands, western Mediterranean), consisting of ichnites of small captorhinomorph eureptiles, probably moradisaurines (*Hyloidichnus*) and parareptiles (cf. *Erpetopus*), and bones of two different taxa of moradisaurines. The smallest of the two is not diagnostic beyond Moradisaurinae *incertae sedis*. The largest one, on the other hand, shows characters that are not present in any other known species of moradisaurine (densely ornamented maxillar teeth), and it is therefore described as *Balearosaurus bombardensis* gen. et sp. nov. Other remains found in the same outcrop are identified as cf. *Balearosaurus bombardensis* gen. et sp. nov., as they could also belong to the newly-described taxon. This species is sister to the moradisaurine from the lower Permian of the neighbouring island of Mallorca, and is also closely related to the North American genus *Rothianiscus*. This makes it possible to suggest the hypothesis that the Variscan mountains, which separated North America from southern Europe during the Permian, were not a very important palaeobiogeographical barrier to the dispersion of moradisaurines. In fact, mapping all moradisaurine occurrences known so far, it is shown that their distribution area encompassed both sides of the Variscan mountains, essentially being restricted to the arid belt of palaeoequatorial Pangaea, where they probably outcompeted other herbivorous clades until they died out in the late Permian.

Captorhinids were a clade of small to medium-sized early eureptiles that became widespread on Laurasia and Gondwana during the Permian. The earliest known member of the group, of small size and with a single-rowed dentition well suited for insectivory, lived in North America during the late Carboniferous (Müller & Reisz 2005; Reisz *et al.* 2016). Captorhinids radiated during the early Permian, maintaining small forms with a single row of teeth that likely fed on insects or even on smaller tetrapods (*e.g.*, Brocklehurst 2017; Modesto *et al.* 2018 and references therein), which coexisted with other small to medium-sized forms that developed other food processing styles. Some of those species were omnivorous, with teeth arranged in a single row or with several rows of teeth oblique to the jaw margins (Modesto *et al.* 2007; LeBlanc & Reisz 2015; Brocklehurst 2017; Reisz *et al.* 2020), whereas others were high-fibre herbivores, always with multiple rows of teeth arranged more or less parallel to the jaw margins (Dodick & Modesto 1995; Reisz & Sues 2000; Modesto *et al.* 2014, 2019; LeBlanc *et al.* 2015; Brocklehurst 2017). This last group has been classified in a subfamily of their own, the Moradisaurinae Ricqlès & Taquet, 1982.

Moradisaurines showed a wide range of sizes, from very small species with a skull length of about 25 mm (Olson 1970), to medium-sized species with a skull length of about 450 mm (Ricqlès & Taquet 1982; Modesto *et al.* 2019). All of them possessed tooth plates with several tooth rows on the dentary and on the maxilla, well suited for high-fibre herbivory (*e.g.*, Dodick & Modesto 1995; Reisz & Sues 2000; LeBlanc *et al.* 2015). In fact, some representatives of both small and medium-sized forms have been inferred to be able to produce a propalinal motion of the lower jaw during food processing (Dodick & Modesto 1995; Modesto *et al.* 2007, 2014, 2019), which enabled them to efficiently grind and shred the plant material on which they fed. The number of rows and teeth per row were variable among the different species and throughout ontogeny (*e.g.*, LeBlanc & Reisz 2015; Jung & Sumida 2017; Modesto *et al.* 2019). In the largest forms, the limb bones became distinctly more robust (*e.g.*, Modesto *et al.* 2019), but not as much as theoretically expected (Romano & Rubidge 2019). In order to reduce the mechanical stress on the limb bones during locomotion, those herbivorous large forms probably moved more slowly (Romano & Rubidge 2019), which did not compromise their ability to obtain plant food, contrarily to smaller captorhinids, which needed to catch their prey.

Ichnites attributed to captorhinomorphs that could be produced by moradisaurines, corresponding to the ichnogenus *Hyloidichnus* Gilmore, 1927, first appear in Sakmarian rocks (lower Permian) of North America (Lucas *et al.* 2013; Schneider, 2020), slightly earlier than the oldest known moradisaurines, which belong to the genus *Captorhinikos* Olson, 1954, reported from the Artinskian to the middle Kungurian (lower Permian) of North and South America (Cisneros *et al.* 2020a and references therein). The genus *Captorhinikos* is currently considered the most basal member and the first high-fibre herbivore of the clade (Brocklehurst 2017;

Modesto *et al.* 2019). Larger herbivorous species started to appear shortly after, represented by the genera *Labidosaurikos* Stovall, 1950 (Kungurian, lower Permian: Dodick & Modesto 1995), *Kahneria* Olson, 1962a (Kungurian/Roadian?, lower/middle Permian: Olson 1962a) and *Rothianiscus* Kuhn, 1961 (Kungurian/Roadian?, lower/middle Permian: Olson 1962a), together with other undetermined specimens from southern North America (Kungurian, lower Permian: Modesto *et al.* 2016) and Mallorca (Artinskian–Kungurian?, lower Permian: Liebrecht *et al.* 2017; Matamales-Andreu *et al.* 2019). This also coincided with an increase in morphological disparity (Brocklehurst 2017), which may have played a part in the ecological success of the group, contributing to the shift to eureptile dominance in the post-Artinskian ichnoassemblages of both Europe and North America (Marchetti *et al.* 2015a, 2019a). There, the ichnogenus *Hyloidichnus* becomes abundant, and in rare cases, it is accompanied by another ichnogenus purportedly produced by large moradisaurines, *Merifontichnus* Gand *et al.*, 2000 (Gand & Durand 2006; Marchetti 2016; Citton *et al.* 2019; Santi *et al.* 2020). In the middle–late Permian, moradisaurines appear represented by small-sized species in eastern Europe (*Gecatogomphius* Vjushkov & Chudinov, 1957, middle Permian: Ivakhnenko 2008), central-east Asia (*Gansurhinus* Reisz *et al.*, 2011, middle–upper Permian: Reisz *et al.* 2011) and North Africa (*Acrodenta* Dutuit, 1976, and other unidentified moradisaurines, upper? Permian: Jalil & Dutuit 1996; Hmich *et al.* 2006), and the largest known species, in central Africa (*Moradisaurus* Taquet, 1969, middle–upper? Permian: Olroyd & Sidor 2017; Modesto *et al.* 2019). The most recent ichnites attributed to moradisaurines belong to the ichnogenus *Hyloidichnus* and were found in upper Permian rocks of North Africa (Voigt *et al.* 2010).

As evidenced by some of the works cited above, the record of body fossils of moradisaurine captorhinid eureptiles in southern Europe was hitherto restricted to the island of Mallorca (Balearic Islands, western Mediterranean). Liebrecht *et al.* (2017) described a fragment of maxilla and parts of the palate of a large moradisaurine, which confirmed the presence of this clade on the island, previously inferred from tracks (Calafat *et al.* 1986, 1986–1987; Calafat 1988; Gand *et al.* 2010; Matamales-Andreu *et al.* 2019). Both the bones and the tracks were found in the Port des Canonge Unit, the age of which is at present unclear and under study, preliminarily dated as lower Permian (Artinskian or Kungurian) (Matamales-Andreu *et al.* 2019). Nevertheless, from the Permian beds of the neighbouring island of Menorca, some authors (Pretus & Obrador 1987; Carmona 2004) had also reported large bones of unidentified tetrapods, which had not been studied in detail so far.

The first report of vertebrate remains on Menorca was published by Pretus & Obrador (1987), illustrating a large scapula found *ex situ*. That and other bones, herein revised, were the object of the preliminary work of Carmona (2004), who suggested that two of the fossil vertebrae belonged to a large and a small species of indeterminate seymouriamorphs. However, it is worth

noting that Carmona (2004) did not consider all the bones that had been collected until then, because some of them had yet to be prepared.

The present work resumes the study of tetrapod bone remains from the Permian of Cala del Pilar–Pla de Mar section (Menorca, Balearic Islands, western Mediterranean), re-assigning all of them to moradisaurine captorhinid eureptiles. This includes the detailed description of all the material present in old collections except for the scapula figured by Pretus & Obrador (1987), which is currently housed in a private collection and preparation required to properly study it has not been possible. Moreover, new ichnological material found at the outcrop is also studied. Unfortunately, new prospection/excavation campaigns have not been carried out due to administrative setbacks. Nevertheless, this study aims to shed light on the hitherto poorly described tetrapod fossils of this site, characterising a new locality of Permian palaeoequatorial faunas.

1. Geological and geographical context

Menorca is the northeasternmost island of the Balearic Archipelago, located at the western Mediterranean. Even as an extension towards the NE of the Betic Orogen, Menorca is quite different from the rest of the Balearic Islands in structural and stratigraphic terms (Bourrouilh 1973; Vera *et al*. 2004; Sàbat *et al*. 2018). Geologically, the island is neatly divided into two main regions: Migjorn, at the S, where a post-orogenic upper Miocene cover is largely dominant; and Tramuntana, at the N, with older materials that broadly span from the Lochkovian (Lower Devonian) to the Rupelian (lower Oligocene) (Bourrouilh 1973, 1983; Vera *et al*. 2004; Martin-Closas & Ramos 2005) (Fig. 1A). The Permian red-beds studied in the present paper, framed between two erosive surfaces, lay within the latter structural unit. They are unconformably disposed over the underlying Devonian or Carboniferous rocks, and the top of their sequence is eroded and overlain by the Lower–Middle Triassic *Buntsandstein* facies (Gómez-Gras 1987, 1992, 1993; Rosell *et al*. 1988, 1989a, 1989b; Bercovici *et al*. 2009; Linol *et al*. 2009). Those beds were first attributed to the upper Permian by Bourrouilh (1973, 1983) and were subsequently studied by Pomar-Gomà (1979), Obrador (1983), Martí *et al*. (1985), Rodríguez-Perea *et al*. (1987), Arribas *et al*. (1990), Brandes & Tiedt (1991), Gómez-Gras (1987, 1992, 1993), Rosell *et al*. (1988, 1989a, 1989b), Broutin *et al*. (1992), Gómez-Gras & Alonso-Zarza (2003), Bercovici *et al*. (2009), Linol *et al*. (2009) and Borruel-Abadía *et al*. (2019).

Despite of all these detailed works, the precise palaeogeographic position of Menorca before the Alpine orogeny is still a matter of discussion. During the late Carboniferous–early Permian, the extensional collapse of the Variscan orogen in Iberia and neighbouring regions opened many rift basins, which were filled with continental sediments until the Middle Triassic

(López-Gómez *et al*. 2019a). Some authors (Gómez-Gras 1992, 1993; Sàbat *et al*. 2018) have argued that the Menorcan sections have a sedimentary evolution that is somewhat reminiscent to that of the basins of the SW of the Catalan Coastal Ranges, in the eastern margin of the Iberian Peninsula. However, the palaeocurrent directions of the Permian and Triassic of Menorca point generally towards the SW (Linol *et al*. 2009), whereas in the Iberian Peninsula the trend is towards the SE (López-Gómez & Arche 1987, 1992; Arche & López-Gómez 1992), and therefore it is unlikely that they were part of a same fluvial system or (sub)basin. The most probable scenario with the data available today is that the Menorcan basin was relatively independent from the other basins of Iberia, including that of the neighbouring island of Mallorca. In any case, the Menorcan basin was probably located very close to the equator throughout the Permian, approximately in a latitude of 4º N (Scotese 2014), at the western margin of the Palaeotethys ocean (Bercovici *et al*. 2009; Linol *et al*. 2009). The climate was tropical, alternating arid and hot seasons with rainy seasons (Gómez-Gras & Alonso-Zarza 2003; Bercovici *et al*. 2009; Roscher *et al*. 2011).

Gómez-Gras (1987) described three lithostratigraphic units for the Permian of Menorca (informally named P1, P2 and P3), which were revised by Rosell *et al.* (1988, 1989a, 1989b), Gómez-Gras (1992, 1993), Bercovici *et al*. (2009) and Linol *et al*. (2009). For the present paper, one stratigraphic section has been logged in detail at the cliffs between Cala del Pilar and Pla de Mar (Fig. 1B–C; Supplementary Material 1), encompassing the three lithostratigraphic units.

1.1. Palaeoenvironment and climatic conditions

The palaeoenvironments of the Permian recorded in Cala del Pilar–Pla de Mar section changed through time, responding to the evolution of the basin and its climatic conditions. A review of the three main lithostratigraphic units, based on the works of Gómez-Gras (1987, 1992, 1993), Rosell *et al.* (1988, 1989a, 1989b), Gómez-Gras & Alonso-Zarza (2003), Bercovici *et al*. (2009), Linol *et al.* (2009) and new data collected for the present study, is offered here:

In the studied section, the P1 unit consists of 4–6 m of crudely bedded, coarse breccias with intercalated sandstones, overlaying the angular, erosive boundary with the Carboniferous *Culm* facies. In the first stages of rifting, when the subsidence rates are high, alluvial/colluvial fans transverse to the main axis of the basin usually develop near the footwall scarp (*e.g.*, Speksnijder 1985; Miall 2006; Franzel *et al*. 2020 and references therein). The P1 unit is here interpreted as one of such deposits, and the formation of calcareous mature palaeosols on top of each of the breccia beds (Gómez-Gras & Alonso-Zarza 2003; Bercovici *et al*. 2009) attests that the depositional events that formed this unit were multiple, separated in time and under a climate with periods of very low precipitation (Gómez-Gras & Alonso-Zarza 2003). Apart from rhizocretions, no fossils have been reported from the P1 unit so far.

In the studied section, the P2 unit consists of about 150 m of massive lutites with sporadic intercalations of sandstones with climbing ripples and, rarely, microbreccias of reworked pedogenic calcretes. This unit represents a playa lake palaeoenvironment (as defined by Briere 2000) in which lutites from overbank flows were deposited (Bercovici *et al.* 2009). Throughout the sequence, there is an alternation of 1–12 m-thick lutitic packs with 0.25–1.5 m-thick intervals that are more resistant to the erosion, with immature palaeosols and/or mud cracks. The former correspond to the deposition of fine sediments during high water table periods, whereas the latter reflect intervals of desiccation of the playa lakes and subsequent formation of mud cracks and incipient palaeosols. Appearing between those, there are sandstone and microbreccia beds with geometries ranging from lenticular (channelled flow) to tabular (unconfined flow), representing crevasse splays and sheetfloods that reworked the floodplains in sporadic heavy rain events (Gómez-Gras & Alonso-Zarza 2003). The fossil content of this unit consists of rhizocretions developed in different types of palaeosols (Bercovici *et al.* 2009), and bones and bone fragments that have been observed in a bed of reworked pedogenic calcrete fragments.

The studied section also comprises the lower 170 m of the P3 unit, consisting of sandstones intercalated with lutites. The bases of the sandstone elements are usually erosive, with a lag of abundant reworked pedogenic calcretes from the floodplains (Gómez-Gras & Alonso-Zarza 2003). Sandstones are organised in two main sequence types: the first, with lateral accreting surfaces and a general upwards decrease of grain size, representing meandering channels, and the second, consisting mostly of tabular beds with horizontal, low-angle cross stratification or climbing ripple lamination, representing sheetflood deposits. Lutites are mostly massive and with a pervasive development of calcareous palaeosols (Bercovici *et al.* 2009). This unit represents a floodplain (playa, as per Briere 2000) with abundant vegetation under a seasonal climate. It was traversed by meandering rivers and, during the rainy seasons, unconfined sheetfloods covered the floodplain. One of the meandering channels, observed at m 301.5–303.5 of the studied section, corresponds to sandstone and breccia beds with abundant lignite lenses and plant debris. This channel was probably abandoned as an oxbow lake, where local reducing conditions favoured precipitation of copper minerals (Crespí & Merino 1998; Llull & Perelló 2013). Other areas of the floodplain were swamped or with a high water table for long time intervals, developing alfisols (Bercovici *et al.* 2009), which have been recognised in several beds of this unit. The most abundant fossils of the P3 unit are rhizocretions (Bercovici *et al.* 2009) and ichnofossils of the *Scoyenia* ichnofacies, including tetrapod tracks. Bones and bone fragments are also locally abundant as part of reworked pedogenic calcrete breccias.

The uppermost part of the P3 unit, cropping out NW of Pla de Mar at Penyals d'Alforinet, has not been considered in the present study because it is separated from the lower part by a very thick covered interval, probably faulted and, moreover, no tetrapod fossils have been found there

so far. It was studied in great detail by Bercovici *et al.* (2009) and Linol *et al.* (2009), and the palaeoenvironments there recorded are similar to those of the rest of the P3 unit.

2. Material and methods

2.1. Collection number abbreviations

FMNH: Field Museum of Natural History, Chicago, Illinois, United States of America.

IPS: Institut Català de Paleontologia Miquel Crusafont (formerly Institut de Paleontologia de Sabadell), Sabadell, Barcelona, Spain.

MBCN: Museu Balear de Ciències Naturals, Sóller, Mallorca, Balearic Islands, Spain.

MNHN: Muséum National d'Histoire Naturelle, Paris, France.

MT: Macar de sa Teula, field code for the rock with the ichnites. It was left in the field (GPS coordinates: 40° 3'9"N 3°58'24"E).

2.2. ZooBank registration of new names

New taxon names have been registered in ZooBank (http://zoobank.org) in order to comply with the rules of the International Code of Zoological Nomenclature for electronic publications (article 8.5.3). The LSID for this publication is: urn:lsid:zoobank.org:pub:8153E0E1-9B66-4C55-89B9-A246195DCD02.

2.3. Stratigraphy and sedimentology

For the stratigraphic and sedimentological study, one section has been logged *in situ*, bed by bed, to a minimum resolution of 1 cm of bed thickness (in 1:25 scale), using a tape measure in well-exposed outcrops and a Jacobs staff for lutite, semi-covered and covered intervals. This section, named Cala del Pilar–Pla de Mar, is here presented in Supplementary Material 1 (in 1:40 scale), and a synthetic version is in Figure 1C (in 1:1160 scale). The recognised sedimentary lithofacies have been classified according to Miall (1985, 2006), Postma (1990), Mack *et al.* (1993), Gómez-Gras & Alonso-Zarza (2003), Bercovici *et al.* (2009) and Linol *et al.* (2009) (Supplementary Material 1).

2.4. Provenance and 3D modelling of tetrapod ichnofossils

The tetrapod ichnites studied in the present work (MT01) were all preserved as natural casts on the surface of an *ex situ* rock found on the beach of Macar de sa Teula. The rock seemed freshly detached from its original bed, which was determined on the outcrop that had to be the one from m 174–179.5 (Fig. 1C), because both the bed and the *ex situ* rock had approximately the same thickness and consisted in very fine sandstones (somewhat silty) with abundant invertebrate burrows and common gleyed patches, unlike other nearby beds. Therefore, its position has been indicated in Figure 1C with a question mark. A photogrammetric 3D model of the ichnites was created (see '3. Systematic palaeoichnology') and then the rock was left at the outcrop.

Photogrammetry is a technique that has recently become widespread in ichnological studies (*e.g.*, Falkingham 2012; Citton *et al*. 2016; Mujal *et al*. 2016a, 2020), making it possible to collect and save information that would otherwise be lost to erosion in the case of big, unmovable rock surfaces. Moreover, it provides an alternative to the confection of artificial casts, which are sometimes hard to make in open environments that are difficult to reach. The present study has broadly followed the same methodology as Mujal *et al*. (2016a, 2020 and references therein), using the open-source software MeshLab v2016.12 (http://meshlab.sourceforge.net/) and ParaView 5.5.0-RC4 64-bit (http://www.paraview.org) to process the meshes. However, to create the mesh, the licensed software Agisoft Photoscan standard v1.1.4. (www.agisoft.com) has been used instead. In order to produce the 3D model, 89 pictures of the surface of MT01 were taken from different angles and distances using a digital camera (Panasonic Lumix DMC-TZ27). Then, they were aligned, and the dense point cloud and the mesh were created. After that, a false-colour height map and contour lines were superimposed on the 3D model, and finally it was drawn on a vector-based graphics design software and measured using the open-source software ImageJ 1.52d (https://imagej.nih.gov/ij/), following the criteria of Leonardi (1987) and Hasiotis *et al.* (2007) (Table 1). The ichnites selected for study correspond to the category "1" of footprint preservation scale by Marchetti *et al.* (2019b), that is, relatively poorly-preserved ichnites missing some diagnostic structures (*i.e.*, some digits). The other ichnites present on the slab scored a "0", that is, their preservation was very poor (Marchetti *et al.* 2019b), so they could not be studied.

The 3D models herein studied are archived and freely available in MorphoSource (https://www.morphosource.org/) with the following DOI: MT01-1 and MT01-2 (https://doi.org/10.17602/M2/M367858), MT01-10 (https://doi.org/10.17602/M2/M367864) and MT01-13 (https://doi.org/10.17602/M2/M367870).

2.5. Phylogenetic analysis

The phylogenetic analysis was performed using a modified version (Supplementary Material 2) of the matrix of Cisneros *et al.* (2020a), mainly with changes introduced by Modesto *et al.* (2019) and Brocklehurst (2020). All character state changes for *Captorhinikos chozaensis* were applied following Modesto *et al.* (2019), except for their character '72' (here character '73') as there was no state 2 (see character list in Modesto *et al.* 2019). Character states for *Moradisaurus* were also recoded following Modesto *et al.* (2019). The rest of character state changes listed by Modesto *et al.* (2019) had already been applied in the matrix of Cisneros *et al.* (2020a). MBCN15730 (the moradisaurine from Mallorca) and *Kahneria* were added to the matrix with the character state codes of Brocklehurst (2020), modifying the following: character '10' of the matrix used by Brocklehurst (2020) was redefined into two characters by Cisneros *et al.* (2020a), so they are now in both cases character '10' with state 1 and character '11' with state 1. Character '42' of MBCN15730 (character '41' in Brocklehurst 2020) was changed from 1 to ?, as the ventral side of the palatine is not visible on the specimen. *Balearosaurus bombardensis* gen. et sp. nov. and the other indeterminate small moradisaurine from Menorca studied in the present work have been coded first-hand. For the final analysis, both the indeterminate small moradisaurine from Menorca and MAP PV664 (Moradisaurinae indet.) from Brazil (Cisneros *et al.* 2020a) were removed because of their large amount of missing data, which caused significant polytomies in the Moradisaurinae. Phylogenetic analysis was run using PAUP* v.4.0 (Swofford 2003) as a branch-and-bound search with parsimony as the optimality criterion, unordered and unweighted characters and with branches collapsing when their maximum length was zero. Then, a strict consensus tree was computed, and bootstrap support values were calculated with 1000 repetitions, not showing values under 50.

3. Systematic palaeoichnology

Ichnogenus *Hyloidichnus* Gilmore, 1927

***Hyloidichnus* isp.**

(Fig. 2A–D; Table 1)

Studied material. MT01-1, MT01-2, MT01-3, MT01-4, natural cast of a partial trackway with a right manus pes set, a left pes imprint and a right pes imprint. MT01-5, natural cast of an isolated left manus imprint. MT01-10, natural cast of a left ?pes imprint. Most of the other footprints of the same surface (MT01-6, MT01-7, MT01-8, MT01-9, MT01-11, MT01-12) may also belong to this ichnogenus given their similar size and general shape but their preservation is too incomplete. All of them were found on an *ex situ* boulder at Macar de sa Teula, attributable

to the m 174–179.5 of Cala del Pilar–Pla de Mar section, P3 Unit, indeterminate Permian, Menorca, Balearic Islands, western Mediterranean.

Description. Pes imprints semiplantigrade, pentadactyl, probably slightly longer (26.4 mm) than wide. The most deeply imprinted parts are digits I and II (medial functional prevalence of the autopodia). The digit imprints radiate from the sole and are relatively slender and straight, with some tips ending in pointed claw traces. The relative length of the preserved digit imprints can be ordered as follows (MT01-1): I<II<III<IV (digit V imprint is not preserved). The sole is anteroposteriorly short, with a well marked posterior margin that is slightly concave. Manus imprint slightly smaller than pes imprint, semiplantigrade, pentadactyl, wider than long. The most deeply imprinted part is the distal region of digit IV, but digits I–III are not preserved so it is not possible to evaluate the functional prevalence of the autopodia. The digit imprints radiate from the palm and are straight and rather short, with tips ending in pointed claw traces. Given the faint imprints of the two available manus (MT01-2 and MT01-5), the relative length of the preserved digit imprints cannot be established, although digit IV appears to be the longest. Acute divergence angle between digit IV–V imprints (21.4º). Palm anteroposteriorly short, with a well-marked posterior margin that is very slightly concave. The imprints of the basal parts of all the digits are well defined, and are the deepest imprinted areas of the sole. Quadrupedal trackway with a simple alternating pattern, with a pace angulation of 71.86º for the pedes. The pes imprints are almost parallel to the midline (divarication of 5º), whereas the manus imprints are strongly rotated inwards (divarication of 44.6º) and seem to be slightly smaller than those of the pes. The pace of the pes ranges between 64.6–69.4 mm, the length of the pace of the pes ranges between 35.4–43.3 mm, and the width of its pace is of 54.0 mm. The interpes distance is of 39.9 mm, and the manus-pes distance is of 12.9 mm.

Remarks. The following combination of characters allows to assign these footprints to *Hyloidichnus* (see Gand 1988; Voigt 2005; Voigt *et al.* 2010; Marchetti 2016; Marchetti *et al.* 2020a; Logghe *et al.* 2021): (1) manus imprints slightly smaller than those of the pedes, (2) orientation of pes imprints parallel to the midline, (3) manus imprints rotated inwards, (4) manus imprint located internally to the pes imprint, (5) acute angle between manus digit IV–V imprints, (6) digit imprints with clawed tips, (7) straight and radiating digits in both the pes and the manus imprints, (8) short sole/palm imprints, (9) ectaxonic tracks and (10) medial-lateral decrease in relief of the track imprints. However, the incomplete preservation of the manus imprints and the trackway precludes any ichnospecies-level assignation. Captorhinomorph eureptiles, and more specifically captorhinids and moradisaurine captorhinids, have been deemed as its most probable trackmakers (*e.g.*, Gand 1988; Haubold 2000; Gand & Durand 2006; Voigt *et al.* 2010; Logghe *et al.* 2021), and this ichnogenus has been found from the Sakmarian (lower Permian) to the Wuchiapingian (upper Permian) (*e.g.*, Lucas 2019; Schneider *et al.* 2020; Logghe *et al.* 2021).

Ichnogenus *Erpetopus* Moodie, 1929

cf. *Erpetopus* isp.

(Fig. 2A–B, E; Table 1)

Studied material. MT01-13, a natural cast of an isolated right ichnite, possibly a manus imprint. Found on an *ex situ* boulder at Macar de sa Teula, attributable to the m 174–179.5 of Cala del Pilar–Pla de Mar section, P3 Unit, indeterminate Permian, Menorca, Balearic Islands, western Mediterranean.

Description. Semiplantigrade, pentadactyl ichnite, slightly wider (11.5 mm) than long (10.9 mm). The most deeply imprinted parts are the bases of the digit imprints, and, especially, those of digits II and V. The digit imprints are thin and those of digits II–IV are distinctly curved inwards distally, whereas the imprints of digits I and V are somewhat straight. Although some of the digit tip imprints undoubtedly have drag traces (I and V), others show an slightly expanded tip that may have corresponded to claw traces (II–IV). The relative length of the digit imprints can be ordered as follows: V<I<II<III<IV. The divergence angles of digit IV–V imprints is high (95.3º), and that of the digit I–V imprints forms a clearly obtuse angle (161.5º). The sole is anteroposteriorly short, concave and well-imprinted posteriorly.

Remarks. MT01-13 can be assigned to *Erpetopus* because of the following combination of characters (Marchetti *et al.* 2014): (1) pes slightly wider than long, (2) slender, curved digit imprints with clawed tips, (3) digit imprints with overlapping digit bases, typical of parareptiles (Marchetti *et al.* 2020b), (4) short digit V imprint, (5) high IV–V divergence, (6) high I–V divergence, (7) small size, less than 20 mm. The most probable trackmakers for *Erpetopus* are acleistorhinid and nyctiphruretid parareptiles, and this ichnogenus has been found from the middle Artinskian (lower Permian) to the Wuchiapingian (upper Permian), being the reference ichnotaxon for the *Erpetopus* footprint biochron (*e.g.*, Lucas 2019; Cisneros *et al.* 2020b; Schneider *et al.* 2020).

4. Systematic vertebrate palaeontology

Reptilia Laurenti, 1768

Eureptilia Olson, 1947

Family Captorhinidae Case, 1911

Subfamily Moradisaurinae Ricqlès & Taquet, 1982

Genus *Balearosaurus* gen. nov.

Type and only included species. *Balearosaurus bombardensis* gen. et sp. nov.

Origin of the name. Combination of *Balearo-*, as it was found in the Balearic Islands, and *-saurus*, Latin for 'lizard'.

Diagnosis. As for the type species.

Balearosaurus bombardensis gen. et sp. nov.

(Fig. 3A–F)

Type specimen. holotype IPS35597 (fragment of right maxilla and palatine), Cala del Pilar–Pla de Mar section, P3 Unit, indeterminate Permian, Menorca, Balearic Islands, western Mediterranean.

Origin of the name. Because most of the fossils here considered to belong to this species were found in the coastal zone called Sa Bombarda (Menorca, Balearic Islands, western Mediterranean).

Studied material. IPS35597 (fragment of right maxilla and palatine), from an *ex situ* rock at Punta des Carregador, attributable to m 149.5 of Cala del Pilar–Pla de Mar section. From the P3 Unit, indeterminate Permian, Menorca, Balearic Islands, western Mediterranean.

Diagnosis. Large moradisaurine captorhinid eureptile with a maxilla with at least three rows of cylindrical teeth that possess an external ornamentation based on longitudinal thin ridges and furrows.

Description. Fragment of right maxilla and palatine of 67.0 mm of maximum anteroposterior length, 25.6 mm of maximum labiolingual width and 27.1 mm of maximum dorsoventral height. No sutures are visible. Three rows of alveoli can be observed: the one in the lingual side shows traces of six alveoli, all of them sectioned. Some still have remains of thecodont teeth attached. The middle row has also six partially covered alveoli. The labial row has five preserved alveoli, three of which are also sectioned and two that are covered by matrix. All of them have a similar size (maximum diameter of 6.4–7.4 mm), and are arranged diagonally to each other. Horizontally on the occlusal side of the maxilla there is a partial isolated cylindrical tooth. Its diameter (7.8 mm) agrees with that of the surrounding alveoli, and its outer surface is covered by an ornamentation consisting of numerous and very thin longitudinal furrows and ridges (Fig. 3D3). On the dorsal side of the maxilla there is a flat surface corresponding to the palatine, tilted 27.3° towards the medial part of the cranium.

Remarks. The maxilla clearly agrees with those of large moradisaurine captorhinid eureptiles. IPS35597 shows at least three parallel rows of teeth; the presence of several longitudinal rows of teeth, organised approximately parallel to the jaw margins, is a diagnostic character of Moradisaurinae (Vjushkov & Chudinov 1957; Olson 1962a, 1962b, 1965; Ricqlès & Taquet 1982; Ricqlès & Bolt 1983; Jalil & Dutuit 1996; Ivakhnenko 2008; Reisz *et al.* 2011; Modesto *et al.* 2014, 2016, 2019; LeBlanc & Reisz 2015; LeBlanc *et al.* 2015; Jung & Sumida 2017). The maxillary teeth are of a similar diameter than that of the largest members of the subfamily, such as *Labidosaurikos* (see Dodick & Modesto 1995), *Moradisaurus* (see Ricqlès & Taquet 1982; Modesto *et al.* 2019), *Rothianiscus* (see Olson 1962a, 1965), the unidentified tooth plates from the 'KB' locality of Texas (Modesto *et al.* 2016) and Mallorca (Liebrecht *et al.* 2017). However, the teeth of all the species in those genera have a smooth surface, devoid of any kind of ornamentation (Olson 1962a, 1965; Ricqlès & Taquet 1982; Dodick & Modesto 1995; Modesto *et al.* 2016, 2019; Liebrecht *et al.* 2017), contrarily to what can be observed on the isolated tooth on the surface of the maxilla in IPS35597, which is traversed by numerous longitudinal furrows and ridges. Only the *Captorhinikos* sp. described by Cisneros *et al.* (2020a: fig. 2) has small furrows and ridges on some teeth, but they seem to be restricted on the base of the crown, contrarily to the isolated tooth of IPS35597, which has a much denser ornamentation that completely covers the preserved surface of the tooth.

The phylogenetic analysis (Fig. 4) places *B. bombardensis* as a derived species within the moradisaurine captorhinids, sister to the undetermined moradisaurine of the neighbouring island of Mallorca, based mostly on the low number of tooth rows. Those two, in turn, are a sister clade of the North American *Rothianiscus*, a genus of large forms with also relatively few rows of teeth, similarly to the Balearic species.

cf. *Balearosaurus bombardensis* gen. et sp. nov.

(Figs. 5–6)

Studied material. IPS35588 (chevron?), IPS35590 (middle caudal vertebra), IPS35592 (anterior dorsal vertebra), IPS35598 (distal fragment of left jaw), IPS120163 (right ilium), IPS120164 (left pubis) and IPS120165 (proximal epiphysis of left tibia), all found in close association in an *ex situ* rock at Sa Bombarda, attributable to m 226–227 of Cala del Pilar–Pla de Mar section. All of them come from the P3 Unit, indeterminate Permian, Menorca, Balearic Islands, western Mediterranean.

Description. IPS35598 (Fig. 5A–F): Distal fragment of left jaw of 66.5 mm of maximum anteroposterior length, 30.9 mm of maximum labiolingual width and 35.4 mm of maximum

dorsoventral height. No sutures are visible. The anterior and posterior ends are broken off, and the occlusal region and part of the lingual and ventral sides are strongly abraded. Although the teeth are missing, one row of five alveoli, which are hemiellipsoidal in shape, can be observed. The first two alveoli are tilted anteriorly, whereas the other three point dorsally. All the alveoli are relatively small (5.7–6.1 mm of maximum diameter) except for the fourth, which is clearly the largest (15.2 mm of diameter), and must certainly have born a large caniniform. Given the symmetrical shape of the alveoli, the mode of attachment of the teeth was thecodont. In dorsal aspect, the jaw is narrowest at its anterior end, and its lingual side expands considerably near the largest alveolus. In labial aspect, the surface is rather flat, and it is traversed by several shallow grooves. In ventral aspect, it possesses a longitudinal groove.

IPS35592 (Fig. 5G–L): Anterior dorsal vertebra of 92.0 mm of height, 93.8 mm of maximum width and 53.0 mm of maximum length. Anteroposteriorly compressed, amphicoelous pleurocentrum of 36.2 mm of height, 42.0 mm of width and 26.8 mm of length, its axis slanting 24º anteriorly with respect to the horizontal. The outline of the pleurocentrum is circular in anteroposterior view and spool-shaped in lateral view, because the cortical rim is slightly flared outwards laterally and ventrally. In ventral aspect, the pleurocentrum is slightly flattened, and no evidence of a ridge or keel can be observed. The neural canal has a somewhat pentagonal contour, being more rounded in anterior view (10.5 mm high × 14.7 mm wide) than in posterior view (8.4 mm high × 13.9 mm wide), flattening the dorsal edge of the pleurocentrum. The pedicels are attached dorsolaterally to the pleurocentrum, anteriorly developing a rather shallow, small fossa just above the cortical rim. From the anterior lateroventral sides of the neural canal, two rounded centroprezygapophyseal processes extend laterally on the pedicels, and possess associated infraprezygapophyseal fossae dorsally, just below the edge of the articular surfaces of the prezygapophyses. The neural arch that stands above is notably expanded and swollen, extending out as much as the width of the pleurocentrum. The prezygapophyses extend laterally from the pedicels (each apophysis corresponding to 1/3 of the total width of the vertebra) and are connected to the transverse processes (diapophysis + parapophysis) posterolaterally. The articular surfaces of the prezygapophyses are slightly tilted inwards from the horizontal plane (10º), and possess a faintly convex obovate contour, which is twice as wide laterally than it is anteroposteriorly. From the medial edges of the prezygapophyses, two carinae extend dorsally, converging at the base of the neural spine. The transverse processes are located between the pre- and postzygapophyses, and are tilted 27º from the vertical axis in anteroposterior aspect. The diapophysis is slightly (15%) thicker than the parapophysis, and they are both connected by an osseous lamina with an angle of 13º from the vertical axis in lateral view. Whereas the diapophysis is dorsolaterally detached forming a small process, the parapophysis fuses at midlength of the posterior region of the prezygapophysis, being reduced to a small bulge. The postzygapophyses are located just

behind the diapophyses in anterior view, separated by a rather deep emargination. A small, laterally elongated suprapostzygapophyseal fossa is present anteriorly on the emarginated side. The postzygapophyseal articular facets are slightly tilted inwards (6.5º) from the horizontal plane, and possess a flat surface. The margins of these surfaces are slightly flared outwards, extending as ridges towards the roof of the neural channel, delimiting the postspinal fossa, which possesses a distinct triangular shape. The hypothetical two edges of the base of that triangle appear on the laminae framing it as two small, dorsolaterally elongated centropostzygapophyseal processes. The dorsal outline of the neural arch in anteroposterior aspect is rather flat, only with small undulations corresponding to the two postzygapophyses and the base of the neural spine. The neural spine is very low (10% of the total height in anterior view) and thin (6% of the total width).

IPS35590 (Fig. 5M–R): Middle caudal vertebra of 44.3 mm of preserved height, 24.8 mm of maximum width and 39.8 mm of maximum length. Cylindrical, amphicoelous pleurocentrum of 28.3 mm of height, 24.8 mm of width and 26.7 mm of length, its axis slanting 13.5º anteriorly with respect to the horizontal. The cortical rim is slightly flared outwards, and it bears a conspicuous bulge on the ventral part of the anterior side, located dorsally just between the haemal keels. In ventral aspect, two haemal keels traverse the pleurocentrum, being more prominent on the anterior cortical rim, and decreasing in height towards the posterior end. No clear facets for the haemal arch have been observed. The neural canal has a rectangular contour in anterior view (12.8 mm high × 9.7 mm wide) and is narrower and almost circular in posterior view (8.8 mm high × 10.3 mm wide). In anterior aspect, the neural arch is broken just above the neural canal. Conversely, in posterior aspect, the postzygapophyses can be observed, the right one being complete. It is strongly directed posteriorly and the articular surface is flat and slightly tilted inwards (24.5º). The neural spine is not preserved.

IPS35588 (Fig. 5S–T): Possible fragment of haemal arch (chevron) of 37.5 mm of maximum dorsoventral height, 7.9 mm of lateral width and 14.7 mm of anteroposterior length. Laterally compressed, dorsoventrally elongated fragment, with a rounded anterior margin that becomes thinner posteriorly. Its distal region is broken; its proximal region, corresponding to the articular surface, is not completely ossified and somewhat irregular, forming an angle of about 65.3º respect to the main axis of the bone.

IPS120163 (Fig. 6A–F): Right ilium, with a lateral surface that appears to be smooth and with no trace of the acetabulum. Anteriorly, the bone ends abruptly in a flat, unfinished surface, corresponding to the suture with the pubis. Ventrally and posteriorly, the bone is eroded, as it was the exposed part when it was found, thus missing the sutural surfaces to the ischium and part of that to the pubis. On its medial surface, there is a somewhat oval area of attachment of the sacral ribs, of 66.6–77.1 mm of diameter. It is located anteriorly to the iliac neck; its dorsal margin is

slightly protruding, its anterior margin is somewhat depressed, and its posterior margin is flat and continuous with the rest of the bone. The iliac blade (123.1 mm of length, 72.6 mm of maximum width and 47.6 mm of height) forms an angle of about 63.4º with the posterior part of the bone. Its neck has a semicircular section, dorsally flattened and with a rounded ventral part, and the blade is elongated, dorsoventrally compressed and expanded distally, with a flattened triangular section. Its posterior end has an unfinished, irregular surface.

IPS120164 (Fig. 6G–I): Left pubis consisting of a thin, relatively flat, triangular plate (148.1 mm of maximum anteroposterior length and 142.8 mm of maximum height), which is slightly curved ventromedially. The maximum lateral width is around its posterior-dorsal edge, reaching 32.3 mm. The anterior, dorsal and posterior margins of the plate are either unfinished or broken, whereas the ventral margin becomes progressively thinner and sharp-edged. The obturator foramen has a subtriangular to oval contour (13.5–20.1 mm of height × 12.3–13-3 mm of width), and obliquely pierces the bone from an anterior-dorsal position in the medial side to a posterior-ventral position on the lateral side.

IPS120165 (Fig. 6J–O): Fragment of the proximal epiphysis of a left tibia, of 131.8 mm of maximum proximal-distal length, with an articular surface of 108.5 mm of anteroposterior width and 96.4 mm of mediolateral width. Most of the medial part of the shaft has been eroded, as it was exposed on the surface when the fossil was found. Articular surfaces can be distinguished on the tibial plateau with some degree of confidence, even though there the bone is slightly eroded (or was not completely ossified). In the lateral half of the plateau, there is a somewhat semicircular depression to accommodate the lateral condyle of the femur. Additionally, another (less clear) elongated or lunate depression can be observed on the medial-extensor edges of the plateau, corresponding to the articulation surface for the medial condyle of the femur. In extensor view, the most proximal part of the cnemial crest can be observed, and although it has been mostly eroded, it appears to bear a fairly inconspicuous knob. Moreover, in lateral view, there is a conspicuous ridge about 44.5 mm below the edge of the tibial plateau.

Remarks. All the bone remains here considered were found in close association, albeit not articulated, so given their consistent size and lack of duplicate elements they can all be considered to belong to the same individual. IPS35597, the holotype specimen of *Balearosaurus bombardensis* gen. et. sp. nov., was collected from a lower stratigraphic position, and given its consistent size and taxonomical attribution it could be considered to be conspecific with the remains herein identified as cf. *Balearosaurus bombardensis* gen. et. sp. nov. However, there is no decisive proof that this specimen (mostly represented by postcranial elements) belongs to the same species as the holotype maxilla of *Balearosaurus bombardensis* gen. et. sp. nov., and therefore it is here treated separately under open nomenclature.

Cranial remains clearly agree with those of large moradisaurine captorhinid eureptiles. IPS35598 is conspicuously heterodont, differentiating a caniniform from other smaller teeth, a condition that is not known to occur in the other Permian tetrapods with swollen vertebral neural arches such as seymouriamorphs and diadectomorphs (see below), which have teeth of similar size in the anterior region of the jaws (*e.g.*, Case 1911; Case & Williston 1912; White 1939; Olson 1947; Carroll *et al.* 1972; Berman *et al.* 1987, 1998; Berman & Sumida 1995; Kissel 2010). Conversely, the dentition of moradisaurines does difference relatively small, bullet-shaped teeth and larger caniniforms (Vjushkov & Chudinov 1957; Olson 1962a, 1965; Ricqlès & Taquet 1982; Dodick & Modesto 1995; Ivakhnenko 2008; LeBlanc *et al.* 2015; Modesto *et al.* 2019). However, the fact that IPS35598 is broken and abraded precludes detailed comparison with other species; regardless, it can be stated that the alveolus for the caniniform is approximately as large as that of the largest known captorhinid, *Moradisaurus grandis* Taquet, 1969 (see Ricqlès & Taquet 1982).

Elements of the axial skeleton, especially IPS35592, are also diagnostic of moradisaurines. Swollen vertebral neural arches are found in seymouriamorphs, diadectomorphs, moradisaurine captorhinomorphs and parareptiles (*e.g.*, Olson & Beerbower 1953; Olson 1962a, 1962b, 1979; Olson & Barghusen 1962; Kuhn 1969; Sullivan & Reisz 1999; Modesto *et al.* 2014). Contrarily to the Menorcan material, seymouriamorph anterior dorsal vertebrae show distinct diapophyses that laterally extend past the zygapophyses (White 1939; Sumida 1990). Moreover, in seymouriamorphs, the parapophyses are located on the intercentra (White 1939; Sumida 1990), whereas in IPS35592 they are on the lateral sides of the neural arches, connected to the diapophyses by a thin lamina, a condition that is seen in captorhinomorphs (*e.g.*, Olson 1962a, 1962b; Olson & Barghusen 1962; Sumida 1990; Reisz *et al.* 2011). Dorsal vertebrae of diadectomorphs and parareptiles are also reminiscent of IPS35592, however, they always possess a thickened and dorsally elongated neural spine, and additional articulation facets in the form of the hypantrum-hyposphene complex (Meyer 1860; Stappenbeck 1905; Case 1911; Kuhn 1969; Carroll *et al.* 1972; Sumida 1990; Berman *et al.* 1998; Nyakatura *et al.* 2015). The vertebra studied herein does possess what seem to be paired, small additional articulation facets, but in the form of the centrozygapophyseal processes and fossae, which are by no means comparable to the stout and conspicuous hypantrum-hyposphene of diadectomorphs and parareptiles. Illustration of isolated vertebral remains of moradisaurines is scarce in the literature, but IPS35592 is remarkably similar to the *Rothianiscus* vertebra (FMNH UR 829) illustrated by Olson & Barghusen (1962) (R.M.A., pers. obs.) and to a purported juvenile *Moradisaurus* vertebra, uncatalogued, in the collections of the MNHN (J.F. & R.M.A., pers. obs.).

The elements of the pelvic girdle are slightly different from those of other moradisaurines of which the pelvis is known, such as *Captorhinikos* (see Olson 1962b) and *Rothianiscus* (see

Olson & Barghusen 1962), in that the iliac blade is dorsoventrally flatter and more posteriorly directed in IPS120163. Some smaller captorhinids, such as *Captorhinus* Cope, 1896, do have iliac blades strongly directed posteriorly (see Holmes 2003), but, apart from in its size, they differ from IPS120163 in that the blade is dorsoventrally flattened in the latter.

Moradisaurinae indet.

(Fig. 7)

Studied material. IPS35593 (middle/posterior dorsal vertebra), found in an *ex situ* rock attributable to m 226–227 of Cala del Pilar–Pla de Mar section (the same as the specimens IPS35588, IPS35590, IPS35592, IPS35598, IPS120163, IPS120164 and IPS120165 mentioned above). IPS120166 (proximal fragment of left jaw), collected *in situ* from the bed at m 273–274 of Cala del Pilar–Pla de Mar section. Both of them come from the P3 Unit, indeterminate Permian, Menorca, Balearic Islands, western Mediterranean.

Description. IPS120166 (Fig. 7A–F): Proximal fragment of left jaw of 42.6 mm of maximum anteroposterior length, 13.6 mm of maximum labiolingual width and 26.6 mm of maximum dorsoventral height. Five bones are partially represented in the studied fragment, although only sutures between two pairs of them are visible (prearticular-splenial and angular-prearticular). Three rows of teeth can be observed on a platform on the dentary, overhanging in the lingual side (11.9 mm of maximum labiolingual width and 7.6 mm of maximum dorsoventral height). Four small (2.0 mm of maximum diameter), bullet-shaped teeth are preserved in the labial row. Detailed preparation has not been possible due to its small size and the potential risk of damaging the fossil, but they seem to be conical and somewhat pointed. Four teeth can be distinguished in the middle row, the most posterior of which is clearly larger (5.0 mm of maximum diameter). Two other small teeth have been counted in the lingual row. All of them are arranged diagonally to each other. In labial view, the dentary is rather flat and tilted laterally (38.3°), and its lower two-thirds are ornamented with irregular grooves. Posterior to the teeth plate rises the coronoid process (tilted 48.3° posteriorly), although the suture between the dentary and the coronoid is not visible, and part of the mandibular ramus. In lingual view, just below the tooth plate there is a flat and smooth surface corresponding to the prearticular. In its posterior part, and although it is covered by matrix, there is an area that corresponds to the articular facet of the hemimandible. The ventral edge of the prearticular is connected to the angular below with a distinct suture and a conspicuous angulation of the surface, which becomes almost horizontal. In the most anterior preserved part of the connexion between the prearticular and the angular there is a anteroposteriorly stretched foramen (Meckelian foramen) that connects to the mandibular

canal visible in anterior aspect. Just below this foramen there is a small portion of the splenial, connecting posteriorly and ventrally with the angular by means of a conspicuous suture.

IPS35588 (Fig. 7G–L): Middle/posterior dorsal vertebra of 33.9 mm of height, 38.0 mm of maximum width and 26.9 mm of maximum length. Cylindrical, amphicoelous pleurocentrum of 14.5 mm of height, 14.6 mm of width and 17.2 mm of length, its axis being almost horizontal. The outline of the pleurocentrum is circular in anteroposterior view and spool-shaped in lateral view, because the cortical rim is slightly flared outwards laterally and ventrally. In ventral aspect, there is no evidence of a ridge or keel. The neural canal has a somewhat pentagonal contour in anterior view (7.1 mm of height × 7.9 mm of width) and is covered by matrix in posterior view. The pedicels are attached dorsolaterally to the pleurocentrum supporting the neural arch, which is notably expanded and swollen, extending out as much as the width of the pleurocentrum. The prezygapophyses extend laterally from the pedicels and are connected to the transverse processes posterolaterally. The articular surfaces of the prezygapophyses are essentially horizontal, and are approximately twice as wide laterally than they are wide anteroposteriorly. Transverse processes are located between the pre- and postzygapophyses, and are tilted 23.1° from the vertical axis in anteroposterior aspect. The diapophysis appears to be half as thick as the parapophysis, and they are both connected by an osseous lamina with an angle of 31° from the vertical axis in lateral view. Whereas the diapophysis is dorsolaterally detached forming a small process, the parapophysis fuses at midlength of the posterior region of the prezygapophysis. The postzygapophyses are located just behind the diapophyses in anterior view, separated by a rather deep emargination. A small, laterally-elongated suprapostzygapophyseal fossa is present anteriorly on the emarginated side. The postzygapophyseal articular facets essentially horizontal, possess a flat surface, and their margins are slightly flared outwards. The neural spine is very low (8% of the total height in anterior view) and thin (7% of the total width). In anterior aspect, it continues ventrally as a faint lamina that fades halfway to the neural canal; in posterior aspect, the spine bifurcates ventrally in two thin laminae that delimit the postspinal fossa, which possesses a distinct triangular shape.

Remarks. The fossils here considered come from two beds separated by a thickness of about 50 m. Therefore, they certainly do not belong to the same specimen (the vertebra would belong to a slightly larger animal), but they have been grouped here because they agree in general size and purported taxonomical attribution. The vertebra (IPS35588) shows typical moradisaurine traits and it is essentially a smaller version of IPS35592, very similar to the vertebrae illustrated by Reisz *et al.* (2011). However, it does not belong to a juvenile specimen of cf. *Balearosaurus bombardensis* but to an adult of a distinct, smaller species, as it is completely ossified and there remain no traces of the neurocentral suture. The jaw (IPS120166) is also small, and broadly comparable to that of some genera of small moradisaurines such as *Captorhinikos* (see Olson

1962b; LeBlanc *et al.* 2015; Cisneros *et al.* 2020a), *Kahneria* (see Olson 1962a), *Gecatogomphius* (see Ivakhnenko 2008), *Acrodenta* (see Jalil & Dutuit 1996) and the unidentified tooth plate from the Argana Basin (Jalil & Dutuit 1996). It differs from most of those genera in that IPS120166 only has three rows of teeth in the most proximal part of the jaw, whereas the others have four or more with a comparable or smaller jaw size. *Acrodenta* does have three rows of teeth, and differs from all other moradisaurine captorhinids in the acrodont mode of implantation of its teeth, which are thin and sharply pointed (Jalil & Dutuit 1996). Teeth in IPS120166 are not as thin and pointed as in *Acrodenta*, as they are more similar to the bullet-shaped teeth of *Captorhinikos* or *Kahneria*, and their mode of implantation cannot be observed in the present material. Therefore, it has been identified in open nomenclature.

5. Discussion

5.1. Age attribution

The precise age attribution for each of the Permian units of Menorca remains mostly unresolved. Bourrouilh (1973, 1983) was the first author to carry out a palynological study on those units with a sample collected in the km 16.9 of the road from Es Mercadal to Alaior, which pointed to an upper Permian age (Bourrouilh 1973, 1983). That outcrop was assigned to the lower half of the P3 unit by Rosell *et al.* (1989a, 1989b), who also provided another palynological analysis from an unspecified locality that revealed a 'Thuringian' biofacies (middle–upper Permian). A few years later, Broutin *et al.* (1992) reported yet another palynoassemblage from Pla de Mar, found in the copper mine beds (in m 301.5–303.5 of the log presented here, and thus in the middle part of the P3 unit), and also considered it to belong to the 'Thuringian' biofacies. That palyniferous horizon could not be relocated by Bercovici *et al.* (2009), but they did find more layers that yielded palynomorphs in the uppermost beds of the P3 unit at Penyals d'Alforinet (not considered herein, see '1.1. Palaeoenvironment and climatic conditions' above), arguing a Wordian–Changhsingian stage (middle–uppermost Permian) interval for them. More recent works, such as Bourquin *et al.* (2011) or Borruel-Abadía *et al.* (2019), considered that palynoassemblage to be of lower Wuchiapingian stage (Lopingian, upper Permian) without providing further proof. Then, they inferred that the lower–middle P3 unit was of upper Capitanian stage (Guadalupian, middle Permian), the P2 unit was of Wordian–lower Capitanian stage (Guadalupian, middle Permian) and the P1 unit was of lower Wordian stage (Guadalupian, middle Permian), without presenting specific data or any compelling argument on how this conclusions were reached.

From a review of the literature, it becomes clear that the only interval of the Permian of Menorca that has been confidently dated, albeit in a notably wide range of time, is the middle– upper part of the P3 unit as Wordian–Changhsingian (middle–uppermost Permian) (Bourrouilh

1973, 1983; Rosell *et al.* 1989a, 1989b; Broutin *et al.* 1992; Bercovici *et al.* 2009). Additionally, the ichnological study of the present work has dated the lower part of the P3 unit as middle Artinskian–Wuchiapingian. All other age inferences, especially those for the lower units, are here considered unfounded, as with the present data it is only possible to attribute the P3 unit to an undetermined interval between the middle Artinskian and the Changhsingian (lower–uppermost Permian), lacking any data for units P1 and P2.

5.2. Tetrapod fauna

All the body fossils from the Permian P3 Unit of Cala del Pilar–Pla de Mar section have been identified to belong to the captorhinid eureptile subfamily Moradisaurinae, similarly to most of the ichnological material, which was produced by captorinomorphs, perhaps moradisaurines as well (*Hyloidichnus* isp.) (Fig. 8). The lack of precise age constraints in the case of the Menorcan units limits the possibility of making detailed palaeobiogeographical inferences. Still, this section will explore the possible relationships with all the other similar species.

     5.2.1. Palaeobiogeography of moradisaurine captorhinid eureptiles. The distribution of all known moradisaurine fossils (bones and putative ichnites) throughout the Permian was essentially restricted to low palaeolatitudes between 30ºN and 30ºS (Fig. 9) (the only exception being the *Hyloidichnus* reported from Argentina by Melchor & Sarjeant 2004). Modesto *et al.* (2016) suggested that moradisaurines and caseids replaced diadectids and edaphosaurids as the dominant high-fibre herbivores in the late part of the early Permian because they may have been better suited to thrive in more arid climates. Indeed, from the early Permian to the middle–late Permian, the low-latitude belt of Pangaea shifted from a tropical climate to an arid climate (Tabor & Poulsen 2008). With moradisaurines restricted to intertropical latitudes, the niches as dominant herbivores in temperate and high latitudes were filled, during the middle and late Permian, by taxa of other groups such as dicynodonts, pareiasaurs and some dinocephalians (*e.g.*, Day *et al.* 2015; Bernardi *et al.* 2017; Olroyd & Sidor 2017; Sennikov & Golubev 2017; Marchetti *et al.* 2019c; Viglietti *et al.* 2019). Such latitudinal provincialism was supported by the analysis of Bernardi *et al.* (2017), who showed that the late Permian faunal palaeoassemblages of low latitudes clustered in what were named "tropical faunas", which were clearly distinct from the palaeoassemblages of higher latitudes. This had also been argued by Sidor *et al.* (2005) regarding the singular middle/upper? Permian assemblage of the Moradi Formation of Niger, with relict representatives of Carboniferous temnospondyl clades that were little related to other coeval taxa. The present work adds up to that evidence, as the distribution of moradisaurines, from the early Permian to the late Permian (Fig. 9), supports the hypothesis of a strong latitudinal provincialism, especially isolating the faunas of the most arid, intertropical regions of Pangaea.

Therefore, if central Pangaea was an area that hindered faunal exchanges between temperate latitudes of both hemispheres, the alternative corridors that explain the great similarities between northern and southern temperate faunas should be sought either in the coastal environments, with less harsh climates (Sidor *et al.* 2005), or in the Cathaysian Bridge, which preserved more humid conditions throughout the Permian (Tabor & Poulsen 2008). Brocklehurst *et al.* (2018) argued that, in all cases, the Permian assemblages of Gondwana were more similar to the ones of eastern Laurasia, whereas it seemed that dispersion had been low between Gondwana and western Laurasia (which includes most of the moradisaurine localities). Thus, the most probable explanation was that the Cathaysian Bridge operated as the main dispersal route at least until the Guadalupian (middle Permian), and that the most important dispersal barrier between western Gondwana and western Laurasia were the high mountains of the Variscan orogen (Brocklehurst *et al.* 2018). Among the different clades included in the analysis, eureptiles seemed to be the group least affected by this barrier, as their dispersal and vicariance rates remained relatively stable throughout the period of uplifting of the mountains (Brocklehurst *et al.* 2018). This agrees with the pattern observed in Figure 9 herein, which shows that moradisaurines were present and radiated in both the northern and southern sides of the Variscan mountains from the very beginning of their evolutionary history. Therefore, even though it appears that the arid climatic belt in central Pangaea or the Variscan mountains could have served as a strong obstacle for dispersal of certain tetrapod groups such as amphibians, parareptiles and synapsids (Brocklehurst *et al.* 2018), they provided comfortable environments for a specialised clade such as moradisaurines.

5.2.2. Phylogenetic relationships of moradisaurine captorhinid eureptiles. The phylogenetic tree of the Captorhinomorpha obtained in the present work (Fig. 4) differs in some aspects from those recently published; specifically, it recovers one polytomy in all the species of *Captorhinus*, the genus *Labidosauriscus* and the clade (*Labidosaurus* + Moradisaurinae), and another polytomy including *Captorhinikos valensis*, *Kahneria* and all the other moradisaurines except for *Captorhinikos chozaensis*. The first politomy is probably the result of merging the character matrix of Modesto *et al.* (2019), resulting in a polytomy between *Captorhinus aguti*, *Captorhinus laticeps* and *Captorhinus magnus*, and the character matrix provided by Cisneros *et al.* (2020a), which obtains a polytomy between *Captorhinus kierani*, *Labidosauriscus* and (*Labidosaurus* + Moradisaurinae). In the former, the polytomy is caused by coding changes in *Captorhinikos chozaensis*, which have been verified again in the present work; in the latter, it is caused by the addition of the two recently described taxa *Captorhinus kierani* and *Labidosauriscus richardi*. The second polytomy is obtained as a result of adding *Kahneria* to the matrix; nevertheless, it does not affect the clade (Balearic species + *Rothianiscus*), which is recovered regardless of *Kahneria* being included in the data matrix or not.

A significative topological difference between the trees of Modesto *et al.* (2019) and Cisneros *et al.* (2020a) is in the position of the single tooth-rowed genus *Labidosaurus*. It is recovered outside all the multiple tooth-rowed Moradisaurinae in the former, whereas in the latter it appears between *Captorhinikos chozaensis* and the rest of multiple tooth-rowed moradisaurines. The tree presented in Figure 4 concurs with the tree recovered by Modesto *et al.* (2019). This aspect has important implications for the phylogeny of the Moradisaurinae, making it a clade restricted to the species with several rows of teeth parallel to the jaw margin, implying that high-fibre herbivory evolved only once within the Captorhinomorpha. In any case, the topology within derived moradisaurines remains the same in the three trees, with the lower–middle Permian North American genus *Rothianiscus*, with one species with three rows of teeth in the major part of its tooth plates (Olson 1962a) as sister to the two large species from Mallorca (Liebrecht *et al.* 2017) and Menorca (Fig. 4).

The large moradisaurine from the island of Mallorca was described by Liebrecht *et al.* (2017), based on a fragment of right maxilla and parts of the palate that belonged to an unknown, large species with three rows of teeth. It was initially assumed (Liebrecht *et al.* 2017) to be of upper Permian age based on the work of Ramos & Doubinger (1989), which dated the palynoassemblages of the upper lithostratigraphic unit of the Permian of the island (Pedra de s'Ase Unit) as 'Thuringian', and thus as middle–upper Permian. However, the moradisaurine fossil was collected in the lower unit (Port des Canonge Unit) (Liebrecht *et al.* 2017), which did not have any reliable age attribution. That unit is now currently under study, and has been preliminarily dated as lower Permian (Artinskian–Kungurian) based on its tetrapod ichnological assemblage (Matamales-Andreu *et al.* 2019). Therefore, the unidentified moradisaurine from Mallorca (Liebrecht *et al.* 2017) should be considered of lower Permian age awaiting further available paleontological and geological data.

As stated above, the phylogenetic analysis offered in the present work (Fig. 4) places this taxon as sister to the large captorhinid from the neighbouring island of Menorca described herein, *Balearosaurus bombardensis* gen. et sp. nov. They belong, however, to clearly distinct species, and possibly genera, which can be set apart mostly based on dental characters, as the Mallorcan moradisaurine has smooth, bulbous teeth (Liebrecht *et al.* 2017), whereas in the Menorcan species the teeth are more cylindrical and ornamented with numerous ridges and furrows (Fig. 3). Despite of its great palaeogeographical proximity, it is important to stress that the Permian units of eastern Iberia (including what are now the Balearic Islands) were deposited in small, semi-isolated half-graben basins (*e.g.*, Gómez-Gras 1992, 1993), which probably operated as biogeographical islands for local speciation of some groups such as moradisaurines.

The close relationship of *Rothianiscus* with the two large moradisaurines of the Balearic Islands further supports the hypothesis put forward in '5.2.1. Palaeobiogeography of moradisaurine captorhinid eureptiles', since the former genus has been found in southern North America, which was on the northwestern side of the Variscan mountains, whereas the Balearic Islands were on its southeastern side (Fig. 9). Therefore, the general case made for all Moradisaurinae is here repeated in a smaller scale, with closely related taxa separated by the Variscan mountains, suggesting that they were not a strong barrier to dispersal of eureptiles.

Regarding the small moradisaurine of Menorca described in the present work, which was impossible to determine with the present material, its relationships within the Moradisaurinae are less clear, and will not be discussed here awaiting the discovery of more complete specimens in the future.

6. Conclusions

The present work has characterised, by means of ichnological and osteological data, a palaeoassemblage from an indeterminate Permian of Cala del Pilar–Pla de Mar section (Menorca, Balearic Islands, western Mediterranean) dominated by moradisaurine captorhinid eureptiles. The field study has allowed to locate and characterise the palaeoenvironments of the bone-bearing beds from which some fossils were extracted and preliminarily studied in the 1980s. This, together with an exhaustive review of the literature, has showed that most of the previous age assignations to those deposits were unfounded, as only the uppermost part of the section had been confidently dated as middle/upper Permian. Additionally, from the middle part of the section, ichnites have been discovered and described for the first time in the Permian of Menorca, recognising the ichnogenera *Hyloidichnus*, purportedly produced by captorhinomorph eureptiles, in this case probably moradisaurine captorhinids, and possibly *Erpetopus*, of acleistorhinid or nyctiphruretid parareptile trackmakers. Two taxa of moradisaurines have also been identified by means of the study of all the fossil bones from the middle part of the Cala del Pilar–Pla de Mar section present in historical collections, which has been the main focus of the present work. The smallest of the two has been identified as an indeterminate moradisaurine based on two bones collected from different beds: a fragment of jaw with three rows of teeth, and an isolated dorsal vertebra with typical characters of the group. The largest of the two taxa has been described as *Balearosaurus bombardensis* gen. et sp. nov. based on a fragment of maxilla with at least three rows of bullet-shaped teeth ornamented with ridges and furrows. Another relatively incomplete specimen consisting of cranial, axial and appendicular bones has also been tentatively assigned to the same species. *Balearosaurus bombardensis* gen. et sp. nov. was closely related to the large moradisaurine reported from the neighbouring island of Mallorca, and those two were in turn

phylogenetically related to *Rothianiscus*, a genus of large moradisaurines from the lower–middle Permian of southern North America. This, together with the distribution of all other known moradisaurines, has allowed to put forward the hypothesis that the Variscan mountains were not an important barrier to biogeographical dispersion of moradisaurines, because species of this clade occurred on both sides of the mountains since the earliest members of the group. Moreover, all known moradisaurines lived in palaeolatitudes between 30ºN and 30ºS, in regions where other herbivorous groups more typical of temperate palaeolatitudes have rarely been reported. This suggests that moradisaurines, together with caseids, may have been among the herbivores best suited to thrive in the arid climates of the low latitudes of Pangaea, outcompeting the rest of herbivorous groups until their demise in the late Permian.

7. Acknowledgements

8. Supplementary material

Supplementary material 1: Lithofacies descriptions (Supplementary Table 1) and detailed stratigraphic log of Cala del Pilar–Pla de Mar section.

Supplementary material 2: Matrix data file (.nexus) used in the phylogenetic analysis.

9. References

Arche, A. & López-Gómez, J. 1992. Una nueva hipótesis sobre las primeras etapas de la evolución tectonosedimentaria de la cuenca pérmico-triásica del SE de la Cordillera Ibérica. *Cuadernos de Geología Ibérica* **16**, 115–143.

Benton, M. J. 2008. *When life nearly died. The greatest mass extinction of all time*. Thames & Hudson: London.

Benton, M. J. & Twitchett, R. J. 2003. How to kill (almost) all life: the end-Permian extinction event. *TRENDS in Ecology and Evolution* **18(7)**, 358–365.

Benton, M. J. & Walker, A. D. 1985. Palaeoecology, taphonomy and dating of Permo-Triassic reptiles from Elgin, north-east Scotland. *Palaeontology* **28**, 207–234.

Bercovici, A., Diez, J. B., Broutin, J., Bourquin, S., Linol, B., Villanueva-Amadoz, U., López-Gómez, J. & Durand, M. 2009. A palaeoenvirnomental analysis of Permian sediments in Minorca (Balearic Islands, Spain) with new palynological and megafloral data. *Review of Palaeobotany and Palynology* **158**, 14–28.

Berman, D. S., Reisz, R. R. & Eberth, D. A. 1987. *Seymouria sanjuanensis* (Amphibia, Batrachosauria) from the Lower Permian Cutler Formation of north-central New Mexico and the occurrence of sexual dimorphism in that genus questioned. *Canadian Journal of Earth Sciences* **24**, 1769–1784.

Berman, D. S., Sumida, S. S. & Martens, T. 1998. *Diadectes* (Diadectomorpha: Diadectidae) from the early Permian of Central Germany, with description of a new species. *Annals of Carnegie Museum* **67(1)**, 53–93.

Berman, D. S. & Sumida, S. S. 1995. New cranial material of the rare diadectid *Desmatodon hesperis* (Diadectomorpha) from the late Pennsylvanian of central Colorado. *Annals of Carnegie Museum* **64(4)**, 315–336.

Bernardi, M., Petti, F. M., Kustatscher, E., Franz, M., Hartkopf-Fröder, C., Labandeira, C. C., Wappler, T., van Konijnenburg-van Cittert, J. H. A., Peecook, B. R. & Angielczyk, K. D. 2017. Late Permian (Lopingian) terrestrial ecosystems: A global comparison with new data from the low-latitude Bletterbach Biota. *Earth-Science Reviews* **175**, 18–43.

Borruel-Abadía, V., Barrenechea, J. F., Galán-Abellán, A. B., De la Horra, R., López-Gómez, J., Ronchi, A., Luque, F. J., Alonso-Azcárate, J. & Marzo, M. 2019. Could acidity be the reason behind the Early Triassic biotic crisis on land? *Chemical Geology* **515**, 77–86.

Bourquin, S., Bercovici, A., López-Gómez, J., Diez, J.B., Broutin, J., Ronchi, A., Durand, M., Arché, A., Linol, B. & Amour, F. 2011. The Permian–Triassic transition and the onset of Mesozoic sedimentation at the northwestern peri-Tethyan domain scale: Palaeogeographic maps and geodynamic implications. *Palaeogeography, Palaeoclimatology, Palaeoecology* **299**, 265–280.

Bourrouilh, R. 1973. *Stratigraphie, sédimentologie et téctonique de l'île de Minorque et du Nord-Est de Majorque (Baléares). La terminaison nord-orientale des Cordilleres Bétiques en Méditerranée occidentale*. State Ph.D. dissertation. Université Pierre & Marie Curie, Paris VI: Paris.

Bourrouilh, R. 1983. Estratigrafía, sedimentología y tectónica de la isla de Menorca y del noreste de Mallorca. *Memorias del Instituto Geológico y Minero de España* **99**, 1–672 + 95 pl. + 3 maps.

Brandes, C. & Tiedt, C. 1991. Petrographische Bestandsaufnahme der permotriassischen Sandsteine Menorcas (Balearen, westliches Mittelmeer). *Neues Jahrbuch für Geologie und Paläontologie, Monatshefte* **1991(4)**, 233–242.

Briere, P. R. 2000. Playa, playa lake, sabkha: Proposed definitions for old terms. *Journal of Arid Environments* **45(1)**, 1–7.

Brocklehurst, N. 2017. Rates of morphological evolution in Captorhinidae: an adaptive radiation of Permian herbivores. *PeerJ* **5:e3200**, 1–25.

Brocklehurst, N. 2020. Olson's Gap or Olson's Extinction? A Bayesian tip-dating approach to resolving stratigraphic uncertainty. *Proceedings of the Royal Society B* **287**, 20200154.

Brocklehurst, N., Dunne, E. M., Cashmore, D. D. & Fröbisch, J. 2018. Physical and environmental drivers of Paleozoic tetrapod dispersal across Pangaea. *Nature Communications* **9**, 5216, 1–12.

Broutin, J., Ferrer, J., Gisbert, J. & Nmila, A. 1992. Permière découverte d'une microflore thuringienne dans le faciès saxonien de l'île de Minorque (Baléares, Espagne). *Comptes Rendus de l'Académie des Sciences de Paris*, s. 2 **315**, 117–122.

Buenaventura, A. 2004. *Menorca, Atlas Náutico*. Editorial Menorca S.A.: Maó.

Calafat, F. 1988. *Estratigrafía y sedimentología de la litofacies Buntsandstein de Mallorca*. Bachelor's Thesis. Universitat de Barcelona: Barcelona.

Calafat, F., Fornós, J. J., Marzo, M., Ramos, E. & Rodríguez-Perea, A. 1986. Icnología de vertebrados de las facies Buntsandstein de Mallorca. *In* Cabrera, L. (ed.) *XI Congreso Español de Sedimentología. Libro de Resúmenes*, p. 40.

Calafat, F., Fornós, J. J., Marzo, M., Ramos-Guerrero, E. & Rodríguez-Perea, A. 1986–1987. Icnología de vertebrados de las facies Buntsandstein de Mallorca. *Acta Geològica Hispànica* **21–22**, 515–520.

Carmona, R. 2004. *Estudi d'un seimuriamorfe (Amphibia: Batrachosauria) del Permià superior de Menorca*. Bachelor's Thesis. Universitat de Barcelona: Barcelona.

Carroll, R. L., Kuhn, O. & Tatarinov, L. P. 1972. Teil 5B / Part 5B: Batrachosauria (Anthracosauria) Gephyrostegida–Chronioschida. *In* Kuhn, O. (ed.) *Handbuch der Paläoherpetologie / Encyclopedia of Paleoherpetology*. Gustav Fischer Verlag: Stuttgart and Portland.

Case, E. C. 1911. A revision of the Cotylosauria of North America. *Carnegie Institution of Washington Publication* **145**, 1–121.

Case, E. C. & Williston, S. W. 1912. A description of the skills of *Diadectes lentus* and *Animasaurus carinatus*. *American Journal of Science*, 4th s. **33**, 339–348.

Cisneros, J. C., Angielczyk, K., Kammerer, C. F., Smith, R. M. H., Fröbisch, J., Marsicano, C. A. & Richter, M. 2020a. Captorhinid reptiles from the lower Permian Pedra de Fogo Formation, Piauí, Brazil: the earliest herbivorous tetrapods in Gondwana. *PeerJ* **8:e8719**, 1–21.

Cisneros, J. C., Kammerer, C. F., Angielczyk, K. D., Fröbisch, J., Marsicano, C., Smith, R. M., & Richter, M. 2020b. A new reptile from the lower Permian of Brazil (*Karutia fortunata* gen. et sp. nov.) and the interrelationships of Parareptilia. *Journal of Systematic Palaeontology* **18(23)**, 1939–1959.

Citton, P., Ronchi, A., Maganuco, S., Caratelli, M., Nicosia, U., Sacci, E. & Romano, M. 2019. First tetrapod footprints from the Permian of Sardinia and their palaeontological and stratigraphical significance. *Geological Journal* **54(4)**, 2084–2098.

Contessi, M., Voigt, S. & Bibonne, R. 2018. Permian Tetrapod Footprints from Tunisia. *Ichnos* **25**, 119–127.

Cope, E. D. 1896. The reptilian order Cotylosauria. *Proceedings of the American Philosophical Society* **34**, 436–457.

Crespí, D. & Merino, A. 1998. Contribució al coneixement de les mines de coure situades en el Permo-Trias de Menorca. *Endins* **22**, 119–123.

Day, M. O., Ramezani, J., Bowring, S. A., Sadler, P. M., Erwin, D. H., Abdala, F. & Rubidge, B. S. 2015. When and how did the terrestrial mid-Permian mass extinction occur? Evidence from the tetrapod record of the Karoo Basin, South Africa. *Proceedings of the Royal Society B* **282**, 20150834.

deBraga, M., Mevitt, J. & Reisz, R. R. 2019. A new captorhinid from the Permian Cave System near Richards Spur, Oklahoma and the taxic diversity of *Captorhinus* at this locality. *Frontiers in Earth Science* **7:112**, 1–19.

Dodick, J. T. & Modesto, S. P. 1995. The cranial anatomy of the captorhinid reptile *Labidosaurikos meachami* from the lower Permian of Oklahoma. *Palaeontology* **38(3)**, 687–711.

Dutuit, J. M. 1976. Il est probable que les Rhynchocéphales sont représentés dans la faune du Trias marocain. *Compte-Rendus de l'Académie des Sciences, Paris* **238**, 483–486.

Erwin, D. H. 1994. The Permo–Triassic extinction. *Nature* **367**, 231–236.

Falkingham, P. L. 2012. Acquisition of high resolution three-dimensional models using free, open-source, photogrammetric software. *Palaeontologia Electronica* **15(1)**, 1T:15p.

Franzel, M., Jones, S. J., Meadows, N., Allen, M. B., McCaffrey, K. & Morgan, T. 2020. Basin-scale fluvial correlation and response to the Tethyan marine transgression: An example from the Triassic of central Spain. *Basin Research* **33(1)**, 1–25.

Gand, G. 1988. *Les traces de vertébrés tétrapodes du Permien français: paléontologie, stratigraphie, paléoenvironnements*. Ph.D. dissertation. Université de Bourgogne: Dijon.

Gand, G. 1993. La palichnofaune de vertébrés tétrapodes du basin permien de Saint-Affrique (Aveyron): comparaisons et conséquences stratigraphiques. *Géologie de la France* **1**, 41–56.

Gand, G., Kerp, H., Parsons, C. & Martínez-García, E. 1997. Palaeoenvironmental and stratigraphic aspects of animal traces and plant remains in Spanish Permian red beds (Peña Sagra, Cantabrian Mountains, Spain). *Geobios* **30(2)**, 295–318.

Gand, G., Garric, J., Demathieu, G. & Ellenberger, P. 2000. La palichnofaune de vertébrés tétrapodes du Permien superiéur du bassin de Lodève (Languedoc-France). *Palaeovertebrata* **29**, 1–82.

Gand, G., De La Horra, R., Galán-Abellán, B., López-Gómez, J., Barrenechea, J. F., Arche, A. & Benito, M. I. 2010. New ichnites from the Middle Triassic of the Iberian Ranges (Spain): palaeoenvironmental and paleogeographical implications. *Historical Biology* **22(1–3)**, 40–56.

Gand, G., Tüysüz, O., Steyer, J. S., Allain, R., Sakınç, M., Sanchez, S., Şengör, A. M. C. & Sen, S. 2011. New Permian tetrapod footprints and macroflora from Turkey (Çakraz Formation, northwestern Anatolia): Biostratigraphic and palaeoenvironmental implications. *Comptes Rendus Palevol* **10**, 617–625.

Gand, G. & Durand, M. 2006. Tetrapod footprint ichno-associations from French Permian basins. Comparisons with other Euramerican ichnofaunas. *Geological Society, London, Special Publications* **265**, 157–177.

Gilmore, C. W. 1927. Fossil footprints of the Grand Canyon: second contribution. *Smithsonian Miscellaneous Collections* **80(3)**, 1–78 + 21 pls.

Gómez-Gras, D. M. 1987. *Estratigrafía física y petrología sedimentaria del Pérmico y Buntsandstein de la isla de Menorca*. Bachelor's Thesis. Universitat Autònoma de Barcelona: Barcelona.

Gómez-Gras, D. M. 1992. *El Permotrías de las Baleares, de la Cordillera Costero Catalana y de la vertiente mediterránea de la Cordillera Ibérica: Facies y Petrología Sedimentaria*. Ph.D. dissertation. Universitat Autònoma de Barcelona: Barcelona.

Gómez-Gras, D. 1993. El Permotrías de las Baleares y de la vertiente mediterránea de la Cordillera Ibérica y del Maestrat: Facies y Petrología Sedimentaria (Parte II). *Boletín Geológico y Minero* **104–105**, 467–515.

Gómez-Gras, D. & Alonso-Zarza, A. M. 2003. Reworked calcretes: their significance in the reconstruction of alluvial sequences (Permian and Triassic, Minorca, Balearic Islands, Spain). *Sedimentary Geology* **158**, 299–319.

Hasiotis, S. T., Platt, B. F., Hembree, D. I. & Everhart, M. J. 2007. The Trace-Fossil Record of Vertebrates. *In* William Miller, III (ed.) *Trace Fossils: Concepts, Problems, Prospects*, 196–218. Elsevier.

Haubold, H. 2000. Tetrapodenfährten aus dem Perm – Kenntnisstand und Progress 2000. *Hallesches Jahrbuch für Geowissenschaften, B* **22**, 1–16.

Haubold, H., Hunt, A. P., Lucas, S. G. & Lockley, M. G. 1995. Wolfcampian (Early Permian) vertebrate tracks from Arizona and New Mexico. *New Mexico Museum of Natural History and Science Bulletin* **6**, 135–165.

Hermite, H. 1879. *Études géologiques sur les îles Baléares. Première partie: Majorque et Minorque*. Pichon et Savy: Paris.

Hermite, H. 1888. Estudios Geológicos de las Islas Baleares. *Boletín de la Comisión del Mapa Geológico* **15**, 1–244 + 4 pl.

Heyler, D. & Lessertisseur, J. 1963. Pistes de tétrapodes Permiens dans la région de Lodève (Hérault). *Muséum National d'Histoire Naturelle, C* **11(2)**, 1–100.

Hmich, D., Schneider, J. W., Saber, H., Voigt, S. & El Wartiti, M. 2006. New continental Carboniferous and Permian faunas of Morocco: implications for biostratigraphy, palaeobiogeography and palaeoclimate. *Geological Society, London, Special Publications* **265**, 297–324.

Hminna, A., Voight, A., Saber, H., Schneider, J. W. & Hmich, D. 2012. On a moderately diverse continental ichnofauna from the Permian Ikakern Formation (Argana Basin, Western High Atlas, Morocco). *Journal of African Earth Sciences* **68**, 15–23.

Holmes, R. B. 2003. The hind limb of *Captorhinus aguti* and the step cycle of basal amniotes. *Canadian Journal of Earth Sciences* **40**, 515–526.

Ivakhnenko, M. F. 2008. Podklass Captorhinomorpha [Subclass Captorhinomorpha]. *In* Ivakhnenko, M. F. & Kurotchkin, E. N. (eds) *Iskopaemye pozvonotchnye Rossii i*

sopredel'nykh stran: Iskopaemye reptilii i ptitsy, Tchast' 1 [Fossil vertebrates of Russia and adjacent countries: Fossil reptiles and birds, Part 1], 86–94. GEOS: Moskva.

Jalil, N. E. & Dutuit, J. M. 1996. Permian captorhinid reptiles from the Argana Formation, Morocco. *Palaeontology* **39**, 907–918.

Jung, J. P. & Sumida, S. S. 2017. A juvenile of the multiple-tooth-rowed reptile *Labidosaurikos* (Eureptilia, Captorhinidae, Moradisaurinae) from the Lower Permian of north-central Texas. *PaleoBios* **34**, 1–5.

Kissel, R. 2010. *Morphology, phylogeny, and evolution of Diadectidae (Cotylosauria: Diadectomorpha).* Ph.D. dissertation. University of Toronto: Toronto.

Kuhn, O. 1961. Pars 99. Reptilia (Supplementum 1(2)). *In* Westphal, F. (ed.) *Fossilium Catalogus. I: Animalia*. Uitgeverij Dr. W. Junk: The Hague, Netherlands.

Kuhn, O. 1969. Teil 6 / Part 6: Cotylosauria. *In* Kuhn, O. (ed.) *Handbuch der Paläoherpetologie / Encyclopedia of Paleoherpetology*. Gustav Fischer Verlag: Stuttgart and Portland.

LeBlanc, A. R. H., Brar, A. K., May, W. & Reisz, R. R. 2015. Multiple tooth-rowed captorhinids from the early Permian fissure fills of the Bally Mountain Locality of Oklahoma. *Vertebrate Anatomy Morphology Palaeontology* **1(1)**, 35–49.

LeBlanc, A. R. H. & Reisz, R. R. 2015. Patterns of tooth development and replacement in captorhinid reptiles: a comparative approach for understanding the origin of multiple tooth rows. *Journal of Vertebrate Paleontology* **35(3)**, e919928, 1–13.

Leonardi, G. 1987. *Glossary and Manual of Tetrapod Footprint Palaeoichnology*. Departamento Nacional de Produção Mineral: Brasília.

Liebrecht, T., Fortuny, J., Galobart, À., Müller, J. & Sander, P. M. 2017. A large, multiple-tooth-rowed captorhinid reptile (Amniota: Eureptilia) from the Upper Permian of Mallorca (Balearic Islands, Western Mediterranean). *Journal of Vertebrate Paleontology* **37(1)**, e1251936, 1–6.

Linol, B., Bercovici, A., Bourquin, S., Diez, J. B., López-Gómez, J., Broutin, J., Durand, M. & Villanueva-Amadoz, U. 2009. Late Permian to Middle Triassic correlations and palaeogeographical reconstructions in south-western European basins: New sedimentological data from Minorca (Balearic Islands, Spain). *Sedimentary Geology* **220**, 77–94.

Llull, B. & Perelló, L. 2013. La mineria de coure a Menorca. De la prehistòria a l'actualitat. *Bolletí de la Societat Arqueològica Lul·liana. Revista d'Estudis Històrics* **69**, 75–93.

Logghe, A., Mujal, E., Marchetti, L., Nel, A., Pouillon, J.-M., Giner, S., Garrouste, R. & Steyer, J.-S. 2021. *Hyloidichnus* trackways with digit and tail drag traces from the Permian of Gonfaron (Var, France): New insights on the locomotion of captorhinomorph eureptiles. *Palaeogeography, Palaeoclimatology, Palaeoecology*, 110436. https://doi.org/10.1016/j.palaeo.2021.110436

López-Gómez, J., Alonso-Azcárate, J., Arche, A., Arribas, J., Fernández-Barrenechea, J., Borruel-Abadía, V., Bourquin, S., Cadenas, P., Cuevas, J., De la Horra, R., Díez, J. B., Escudero-Mozo, M. J., Fernández-Viejo, G., Galán-Abellán, B., Galé, C., Gaspar-Escribano, J., Gisbert-Aguilar, J., Gómez-Gras, D., Goy, A., Gretter, N., Heredia-Carballo, N., Lago, M., Lloret, J., Luque, J., Márquez, L., Márquez-Aliaga, A., Martín-Algarra, A., Martín-Chivelet, J., Martín-González, F., Marzo, M., Mercedes-Martín, R., Ortí, F., Pérez-López, A., Pérez-Valera, F., Pérez-Valera, J. A., Plasencia, P., Ramos, E., Rodríguez-Méndez, L., Ronchi, A., Salas, R., Sánchez-Fernández, D., Sánchez-Moya, Y., Sopeña, A., Suárez-Rodríguez, Á., Tubía, J. M., Ubide, T., Valero-Garcés, B., Vargas, H. & Viseras, C. 2019a. Permian-Triassic rifting stage. *In* Vergés, J. & Kullberg, J. C. (coords) *The Geology of Iberia: A Geodynamic Approach. Volume 3: The Alpine Cycle*, 29–112. Springer: Cham.

López-Gómez, J., Martín-González, F., Heredia, N., De la Horra, R., Barrenechea, J. F., Cadenas, P., Juncal, M., Diez, J. B., Borruel-Abadía, V., Pedreira, D., García-Sansegundo, J., Farias, P., Galé, C., Lago, M., Ubide, T., Fernández-Viejo, G. & Gand, G. 2019b. New lithostratigraphy for the Cantabrian Mountains: a common tectono-stratigraphic evolution for the onset of the Alpine cycle in the W Pyrenean realm, N Spain. *Earth-Science Reviews* **188**, 249–271.

López-Gómez, J. & Arche, A. 1987. Evolución sedimentológica de la Unidad «Limos y areniscas de Alcotas». Tramo medio de la Facies Buntsandstein del sector SE de la Rama Castellana de la Cordillera Ibérica (Provincias de Cuenca y Valencia). *Acta Geològica Hispànica* **21–22**, 9–18.

López-Gómez, J. & Arche, A. 1992. Las unidades litoestratigráficas del Pérmico y Triásico Inferior y Medio en el sector SE de la Cordillera Ibérica. *Estudios Geológicos* **48**, 123–143.

Lucas, S. G. 2019. An ichnological perspective on some major events of Paleozoic tetrapod evolution. *Bollettino della Società Paleontologica Italiana* **58(3)**, 223–266.

Lucas, S. G., Krainer, K., Chaney, D. S., DiMichele, W. A., Voigt, S., Berman, D. S. & Henrici, A. C. 2013. The Lower Permian Abo Formation in Central New Mexico. *New Mexico Museum of Natural History and Science Bulletin* **59**, 161–180.

Mack, G. H., James, W. C. & Monger, H. C. 1993. Classification of paleosols. *Geological Society of America Bulletin* **105**, 129–136.

Marchetti, L. 2016. New occurrences of tetrapod ichnotaxa from the Permian Orobic Basin (Northern Italy) and critical discussion of the age of the ichnoassociation. *Papers in Palaeontology* **2(3)**, 363–386.

Marchetti, L., Avanzini, M. & Conti, M. A. 2013. *Hyloidichnus bifurcatus* Gilmore, 1927 and *Limnopus heterodactylus* (King, 1845) from the Early Permian of Southern Alps (N Italy): A New Equilibrium in the Ichnofauna. *Ichnos* **20**, 202–217.

Marchetti, L., Santi, G. & Avanzini, M. 2014. The problem of small footprints in paleoichnology: remarks on the early Permian ichnotaxon *Erpetopus cassinsi*, a local species from southern Alps (northern Italy). *Rivista Italiana di Paleontologia e Stratigrafia* **120(2)**, 129–143.

Marchetti, L., Ronchi, A., Santi, G., Schirolli, P. & Conti, M. A. 2015a. Revision of a classic site for Permian tetrapod ichnology (Collio Formation, Trompia and Caffaro valleys, N. Italy), new evidences for the radiation of captorhinomorph footprints. *Palaeogeography, Palaeoclimatology, Palaeoecology* **433**, 140–155.

Marchetti, L., Ronchi, A., Santi, G. & Voigt, S. 2015b. The Gerola Valley site (Orobic Basin, Northern Italy): A key for understanding late Early Permian tetrapod ichnofaunas. *Palaeogeography, Palaeoclimatology, Palaeoecology* **439**, 97–116.

Marchetti, L., Forte, G., Bernardi, M., Wappler, T., Hartkopf-Fröder, C., Krainer, K. & Kustatscher, E. 2015c. Reconstruction of a Late Cisuralian (Early Permian) floodplain lake environment: Palaeontology and sedimentology of the Tregiovo Basin (Trentino–Alto Adige, Northern Italy). *Palaeogeography, Palaeoclimatology, Palaeoecology* **440**, 180–220.

Marchetti, L., Belvedere, M., Voigt, S., Klein, H., Castanera, D., Díaz-Martínez, I., Marty, D., Xing, L., Feola, S., Melchor, R.N. & Farlow, J. O. 2019b. Defining the morphological quality of fossil footprints. Problems and principles of preservation in tetrapod ichnology with examples from the Palaeozoic to the present. *Earth-Science Reviews* **193**, 109–145.

Marchetti, L., Klein, H., Buchwitz, M., Ronchi, A., Smith, R. M. H., De Klerk, W. J., Sciscio, L. & Groenewald, G. H. 2019c. Permian-Triassic vertebrate footprints from South Africa: Ichnotaxonomy, producers and biostratigraphy through two major faunal crises. *Gondwana Research* **72**, 139–168.

Marchetti, L., Voigt, S., Lucas, S. G., Francischini, H., Dentzien-Dias, P., Sacchi, R., Mangiacotti, M., Scali, S., Gazzola, A., Ronchi, A. & Millhouse, A. 2019a. Tetrapod ichnotaxonomy in eolian paleoenvironments (Coconino and De Chelly formations, Arizona) and late Cisuralian (Permian) sauropsid radiation. *Earth-Science Reviews* **190**, 148–170.

Marchetti, L., Voigt, S., Lucas, S.G., Stimson, M.R., King, O.A. & Calder, J.H. 2020a. Footprints of the earliest reptiles: *Notalacerta missouriensis* – Ichnotaxonomy, potential trackmakers, biostratigraphy, palaeobiogeography and palaeoecology. *Annales Societatis Geologorum Poloniae* **90**, 271–290.

Marchetti, L., Voigt, S., Mujal, E., Lucas, S.G., Francischini, H., Fortuny, J. & Santucci, V.L. 2020b. Extending the footprint record of Pareiasauromorpha to the Cisuralian: earlier

appearance and wider palaeobiogeography of the group. *Papers in Palaeontology* **2020**, 1–23.

Martí, J., Paniello, X., Pomar, L., Ramos, E. & Rodríguez-Perea, A. 1985. El Triásico de las Baleares. *In* Mateu Ibars, F. & Marzo, M. (eds) *II Coloquio de Estratigrafía y Paleogeografía del Pérmico y Triásico de* España, 84–85. La Seu d'Urgell, 23–25 Septiembre 1985. Libro de Resúmenes.

Martin-Closas, C. & Ramos, E. 2005. Palaeogene Charophytes of the Balearic Islands (Spain). *Geologica Acta* **3(1)**, 39–58.

Matamales-Andreu, R., Fortuny, J., Mujal, E. & Galobart, À. 2019. Tetrapod tracks from the Permian of Mallorca (western Mediterranean): preliminary data, biostratigraphic and biogeographic inferences. *In The Palaeontological Association, 63rd annual meeting, 15th–21st December 2019*, 107.

Melchor, R. N. & Sarjeant, W. A. S. 2004. Small amphibian and reptile footprints from the Permian Carapacha Basin, Argentina. *Ichnos* **11**, 57–78.

Meyer, H. von 1860. *Phanerosaurus Naumanni* ans dem Sandstein des Rothliegenden in Deutschland. *Paleontographica* **7**, 248–252 + pl. 27.

Miall, A. D. 1985. Architectural-Element Analysis: a new method of facies analysis applied to fluvial deposits. *Earth-Science Reviews* **22**, 261–308.

Miall, A. D. 2006. *The Geology of Fluvial Deposits: Sedimentary Facies, Basin Analysis, and Petroleum Geology*. 4th ed. Springer: Berlin, Heidelberg, New York.

Michel, L.A., Tabor, N.J., Montañez, I.P., Schmitz, M.D. & Davydov, V.I. 2015. Chronostratigraphy and Paleoclimatology of the Lodève Basin, France: Evidence for a pan-tropical aridification event across the Carboniferous–Permian boundary. *Palaeogeography, Palaeoclimatology, Palaeoecology* **430**, 118–131.

Modesto, S. P., Scott, D. M., Berman, D. S., Müller, J. & Reisz, R. R. 2007. The skull and the palaeoecological significance of *Labidosaurus hamatus*, a captorhinid reptile from the Lower Permian of Texas. *Zoological Journal of the Linnean Society* **149**, 237–262.

Modesto, S. P., Lamb, A. J. & Reisz, R. R. 2014. The captorhinid reptile *Captorhinikos valensis* from the lower Permian Vale Formation of Texas, and the evolution of herbivory in eureptiles. *Journal of Vertebrate Paleontology* **34(2)**, 291–302.

Modesto, S. P., Flear, V. J., Dilney, M. M. & Reisz, R. R. 2016. A large moradisaurine tooth plate from the lower Permian of Texas and its biostratigraphic implications. *Journal of Vertebrate Paleontology* **36(6)**, e1221832, 1–4.

Modesto, S. P., Scott, D. & Reisz, R. R. 2018. A new small captorhinid reptile from the lower Permian of Oklahoma and resource partitioning among small captorhinids in the Richards Spur fauna. *Papers in Palaeontology* **4(2)**, 293–307.

Modesto, S. P., Richards, C. D., Ide, O. & Sidor, C. A. 2019. The vertebrate fauna of the upper Permian of Niger — X. The mandible of the captorhinid reptile *Moradisaurus grandis*. *Journal of Vertebrate Paleontology* **38(6)**, e1531877, 1–14.

Moodie, R. L. 1929. Vertebrate footprints from the Red Beds of Texas. *American Journal of Science* **97**, 352–368.

Moreau, J.-D., Benaouiss, N., Tourani, A., Steyer, J.-S., Laurin, M., Peyer, K., Béthoux, O., Aouda, A. & Jalil, N.-E. 2020. A new ichnofauna from the Permian of the Zat Valley in the Marrakech High Atlas of Morocco. *Journal of African Earth Sciences* **172**, 103973, 1–14.

Mujal, E., Fortuny, J., Oms, O., Bolet, A., Galobart, À. & Anadón, P. 2016. Palaeoenvironmental reconstruction and early Permian ichnoassemblage from the NE Iberian Basin (Pyrenean Basin). *Geological Magazine* **153(4)**, 578–600.

Mujal, E., Fortuny, J., Pérez-Cano, J., Dinarès-Turell, J., Ibáñez-Insa, J., Oms, O., Vila, I., Bolet, A. & Anadón, P. 2017. Integrated multi-stratigraphic study of the Coll de Terrers late Permian–Early Triassic continental succession from the Catalan Pyrenees (NE Iberian Peninsula): A geologic reference record for equatorial Pangaea. *Global and Planetary Change* **159**, 46–60.

Mujal, E., Marchetti, L., Schoch, R. R. & Fortuny, J. 2020. Upper Paleozoic to lower Mesozoic tetrapod ichnology revisited: photogrammetry and relative depth pattern inferences on functional prevalence of autopodia. *Frontiers in Earth Science* **8:248**, 1–23.

Müller, J. & Reisz, R. R. 2005. An early captorhinid reptile (Amniota, Eureptilia) from the Upper Carboniferous of Hamilton, Kansas. *Journal of Vertebrate Paleontology* **25(3)**, 561–568.

Nyakatura, J. A., Allen, V. R., Lauströer, J., Andikfar, A., Danczak, M., Ullrich, H.-J., Hufenbach, W., Martens, T. & Fischer, M. S. 2015. A three-dimensional skeletal reconstruction of the stem amniote *Orobates pabsti* (Diadectidae): analyses of body mass, centre of mass position, and joint mobility. *PLoS ONE* **10(9)**, e0137284, 1–20.

O'Keefe, F. R., Sidor, C. A., Larsson, H. C., Maga, A. & Ide, O. 2005. The vertebrate fauna of the upper Permian of Niger—III, Morphology and ontogeny of the hindlimb of *Moradisaurus grandis* (Reptilia, Captorhinidae). *Journal of Vertebrate Paleontology* **25(2)**, 309–319.

Olroyd, S. L. & Sidor, C. A. 2017. A review of the Guadalupian (middle Permian) global tetrapod fossil record. *Earth-Science Reviews* **171**, 583–597.

Olson, E. C. 1947. The family Diadectidae and its bearing on the classification of reptiles. *Fieldiana: Geology* **11(1)**, 1–53.

Olson, E. C. 1954. Fauna of the Vale and Choza: 9. Captorhinomorpha. *Fieldiana: Geology* **10(19)**, 211–218.

Olson, E. C. 1962a. Late Permian terrestrial vertebrates, U.S.A. and U.S.S.R. *Transactions of the American Philosophical Society* **52(2)**, 1–224.

Olson, E. C. 1962b. Permian vertebrates from Oklahoma and Texas. Part II. — The osteology of *Captorhinikos chozaensis* Olson. *Oklahoma Geological Survey Circular* **59**, 49–68.

Olson, E. C. 1965. New Permian vertebrates from the Chickasha Formation in Oklahoma. *Oklahoma Geological Survey Circular* **70**, 1–70.

Olson, E. C. 1970. New and little known genera and species of vertebrates from the Lower Permian of Oklahoma. *Fieldiana: Geology* **18(3)**, 359–434.

Olson, E. C. 1979. *Seymouria grandis* n. sp. (Batrachosauria: Amphibia) from the middle Clear Fork (Permian) of Oklahoma and Texas. *Journal of Paleontology* **53(3)**, 720–728.

Olson, E. C. & Beerbower, J. R. 1953. The San Angelo Formation, Permian of Texas, and its vertebrates. *The Journal of Geology* **61(5)**, 389–423.

Olson, E. C. & Barghusen, H. 1962. Permian vertebrates from Oklahoma and Texas. Part I. — Vertebrates from the Flowerpot Formation, Permian of Oklahoma. *Oklahoma Geological Survey Circular* **59**, 4–48.

Pomar-Gomà, L. 1979. *The Triassic of the Balearic Islands*. Geology Department, Palma de Mallorca University: Palma.

Postma, G. 1990. Depositional architecture and facies of river and fan deltas: a synthesis. *In* Colella, A. & Prior, D. B. (eds.) *Coarse-Grained Deltas. Special Publications of the International Association of Sedimentologists* **10**, 13–27.

Pretus, J. Ll. & Obrador, A. 1987. Presencia de restos óseos en el Pérmico de Menorca (nota previa). *Bolletí de la Societat d'Història Natural de Balears* **31**, 149–152.

Ramos, A. & Doubinger, J. 1989. Premières datations palynologiques dans le facies Buntsandstein de l'île de Majorque (Baléares, Espagne). *Comptes Rendus de l'Académie des Sciences de Paris*, s. 2 **309**, 1089–1094.

Reisz, R. R., Liu, J., Li, J.-L. & Müller, J. 2011. A new captorhinid reptile, *Gansurhinus qingtoushanensis*, gen. et sp. nov., from the Permian of China. *Naturwissenschaften* **98**, 435–441.

Reisz, R. R., Haridy, Y. & Müller, J. 2016. *Euconcordia* nom. nov., a replacement name for the captorhinid eureptile *Concordia* Müller and Reisz, 2005 (non Kingsley, 1880), with new data on its dentition. *Vertebrate Anatomy Morphology Palaeontology* **3**, 1–6.

Reisz, R. R., MacDougall, M. J., LeBlanc, A. R. H., Scott, D. & Nagesan, R. S. 2020. Lateralized feedins behaviour in a Paleozoic reptile. *Current Biology* **30**, 2374–2378.

Reisz, R. R. & Sues, H.-D. 2000. Herbivory in late Paleozoic and Triassic terrestrial vertebrates. *In* Sues, H.-D. (ed) *Evolution of Herbivory in Terrestrial Vertebrates*, 9–41. Cambridge University Press.

Ricqlès, A. de & Bolt, J. R. 1983. Jaw growth and tooth replacement in *Captorhinus aguti* (Reptilia: Captorhinomorpha): a morphological and histological analysis. *Journal of Vertebrate Paleontology* **3(1)**, 7–24.

Ricqlès, A. de & Taquet, P. 1982. La faune de vertébrés du Permien Supérieur du Niger. I. Le captorhinomorphe *Moradisaurus grandis* (Reptilia, Cotylosauria). Le crane. *Annales de Paléontologie (Vert.-Invert.)* **68**, 33–106.

Rodríguez-Perea, A., Ramos-Guerrero, E., Pomar, L., Paniello, X., Obrador, A. & Martí, J. 1987. El Triásico de las Baleares. *Cuadernos de Geología Ibérica* **11**, 295–321.

Romano, M. & Rubidge, B. 2019. Long bone scaling in Captorhinidae: do limb bones scale according to elastic similarity in sprawling basal amniotes? *Lethaia* **52(3)**, 389–402.

Rosell, J., Arribas, J., Elízaga, E. & Gómez-Gras, D. 1988. Caracterización sedimentológica y petrográfica de la serie roja permo–triásica de la isla de Menorca. *Boletín Geológico y Minero* **99(1)**, 71–82.

Rosell, J., Gómez-Gras, D. & Elízaga, E. 1989a. *Mapa Geológico de España. Escala 1:25.000. Isla de Menorca. Cap Menorca y Ciutadella.* Segunda serie, primera edición. Instituto Tecnológico GeoMinero de España: Madrid.

Rosell, J., Gómez-Gras, D. & Elízaga, E. 1989b. *Mapa Geológico de España. Escala 1:25.000. Isla de Menorca. Cala en Brut i Alaior.* Segunda serie, primera edición. Instituto Tecnológico GeoMinero de España: Madrid.

Sàbat, F., Gelabert, B. & Rodríguez-Perea, A. 2018. Minorca, an exotic Balearic island (western Mediterranean). *Geologica Acta* **16(4)**, 411–426.

Santi, G., Marchetti, L., Schirolli, P. & Ronchi, A. 2020. The Cisuralian tetrapod ichnoassociation from Italy: from historical findings to a standard reference status. *Journal of Mediterranean Earth Sciences* **12**, 39–59.

Scotese, C. R. 2014. Atlas of Middle & Late Permian and Triassic Paleogeographic Maps, maps 43 – 48 from Volume 3 of the PALEOMAP Atlas for ArcGIS (Jurassic and Triassic) and maps 49 – 52 from Volume 4 of the PALEOMAP Atlas for ArcGIS (Late Paleozoic), Mollweide Projection, PALEOMAP Project: Evanston, IL, USA.

Schneider, J. W., Lucas, S. G., Scholze, F., Voigt, S., Marchetti, L., Klein, H., Opluštil, S., Werneburg, R., Golubevb, V. K., Barrick, J. E., Nemyrovska, Y., Ronchil, A., Day, M. O., Silantiev, V. V., Rößler, R., Saber, H., Linnemann, U., Zharinova, V. & Shen, S.-Z. 2020. Late Paleozoic–early Mesozoic continental biostratigraphy — Links to the Standard Global Chronostratigraphic Scale. *Palaeoworld* **29(2)**, 186–238.

Sennikov, A. G., & Golubev, V. K. 2017. Sequence of Permian tetrapod faunas of Eastern Europe and the Permian–Triassic ecological crisis. *Paleontological Journal* **51(6)**, 600–611.

Sidor, C. A., O'Keefe, F. R., Damiani, R., Steyer, J. S., Smith, R. M. H., Larsson, H. C. E., Sereno, P. C., Ide, O. & Maga, A. 2005. Permian tetrapods from the Sahara show climate-controlled endemism in Pangaea. *Nature* **434**, 886–889.

Smith, R. M., Sidor, C. A., Tabor, N. J. & Steyer, J.-S. 2015. Sedimentology and vertebrate taphonomy of the Moradi Formation of northern Niger: A Permian wet desert in the tropics of Pangaea. *Palaeogeography, Palaeoclimatology, Palaeoecology* **440**, 128–141.

Speksnijder, A. 1985. Anatomy of a strike-slip fault controlled sedimentary basin, Permian of the southern Pyrenees, Spain. *Sedimentary Geology* **44**, 179–223.

Stappenbeck, R. 1905. Über *Stephanospondylus* n. g. und *Phanerosaurus* H. v. Meyer. *Zeitschrift der Deutschen Geologischen Gesellschaft* **57**, 380–437.

Stovall, J. W. 1950. A new cotylosaur from North Central Oklahoma. *American Journal of Science* **248(1)**, 46–54.

Sullivan, C. & Reisz, R. R. 1999. First record of *Seymouria* (Vertebrata: Seymouriamorpha) from Early Permian fissure fills at Richards Spur, Oklahoma. *Canadian Journal of Earth Sciences* **36**, 1257–1266.

Sumida, S. S. 1990. Vertebral morphology, alternation of neural spine height, and structure in Permo-Carboniferous tetrapods, and a reappraisal of primitive modes of terrestrial locomotion. *University of California Publications in Zoology* **122**, 1–129 + 3 pls.

Swofford, D. L. 2003. PAUP*. Phylogenetic Analysis Using Parsimony (*and Other Methods). Version 4. Sinauer Associates: Sunderland, Massachusetts.

Tabor, N. J. & Poulsen, C. J. 2008. Palaeoclimate across the Late Pennsylvanian–Early Permian tropical palaeolatitudes: A review of climate indicators, their distribution, and relation to palaeophysiographic climate factors. *Palaeogeography, Palaeoclimatology, Palaeoecology* **268(3–4)**, 293–310.

Taquet, P. 1969. Première découverte en Afrique d'un reptile captorhinomorphe (cotylosaurien). *Comptes Rendus Hebdomadaires des Séances de l'Academie des Sciences Paris*, s. D **268**, 779–781.

Vera, J.-A., Alonso-Chaves, F. M., Andreo, B., Arias, C., Azañón, J. M., Balanyá, J. C., Barón, A., Booth-Rea, G., Castro, J. M., Chacón, B., Company, M., Crespo-Blanc, A., Delgado, F., Díaz de Federico, A., Esteras, M., Estévez, A., Fernández, J., Fornós, J. J., Galindo-Zaldívar, J., García-Casco, A., García-Dueñas, V., García-Hernández, M., Garrido, C. J., Gea, G. A. de, Gelabert, B., Gervilla, F., González-Lodeiro, F., Jabaloy, A., López-Garrido, A. C., Luján, M., Martín-Algarra, A., Martín-Chivelet, J., Martín-Martín, M., Molina, J. M., Morata, D., Nieto, J. M., Obrador, A., O'Dogherty, L., Orozco, M., Pérez-López, A., Pomar, L., Puga, E., Ramos, E., Rey, J., Rivas, P., Rodríguez-Cañero, R., Ruiz-Cruz, M. D., Ruiz-Ortiz, P. A., Sàbat, F., Sánchez-Gómez, M., Sánchez-Navas, A., Sandoval, J., Sanz de Galdeano, C., Soto, J. I., Torres-Roldán, R. L. & Villas, L. 2004.

Capítulo 4. Cordillera Bética y Baleares. *In* Vera, J.-A. (ed.) *Geología de España*, 345–464. Instituto Tecnológico GeoMinero de España: Madrid.

Viglietti, P. A., Smith, R. M., Angielczyk, K. D., Kammerer, C. F., Fröbisch, J., & Rubidge, B. S. 2016. The *Daptocephalus* Assemblage Zone (Lopingian), South Africa: a proposed biostratigraphy based on a new compilation of stratigraphic ranges. *Journal of African Earth Sciences* **113**, 153–164.

Vjushkov, B. P. & Chudinov, P. K. 1957. Otkrytie Kaptorinid v verkhnnej Permi SSSR [Discovery of a captorhinid in the upper Permian of the USSR]. *Doklady Akademii Nauk SSSR* **112(3)**, 523–536.

Voigt, S. 2005. *Die Tetrapodenichnofauna des kontinentalen Oberkarbon und Perm im Thüringer Wald - Ichnotaxonomie, Paläoökologie und Biostratigraphie*. Cuvillier Verlag: Göttingen.

Voigt, S., Hminna, A., Saber, H., Schneider, J. W. & Klein, H. 2010. Tetrapod footprints from the uppermost level of the Permian Ikakern Formation (Argana Basin, Western High Atlas, Morocco). *Journal of African Earth Sciences* **57**, 470–478.

Voigt, S., Lagnaoui, A., Hminna, A., Saber, H. & Schneider J. W. 2011. Revisional notes on the Permian tetrapod ichnofauna from the Tiddas Basin, central Morocco. *Palaeogeography, Palaeoclimatology, Palaeoecology* **302**, 474–483

Voigt, S. & Haubold, H. 2015. Permian tetrapod footprints from the Spanish Pyrenees. *Palaeogeography, Palaeoclimatology, Palaeoecology* **417**, 112–120.

Voigt, S. & Lucas, S. G. 2015. Permian tetrapod ichnodiversity of the Prehistoric Trackways National Monument (south-central New Mexico, USA). *New Mexico Museum of Natural History and Science Bulletin* **65**, 153–167.

Voigt, S. & Lucas, S. G. 2017. Early Permian tetrapod footprints from central New Mexico. *New Mexico Museum of Natural History and Science Bulletin* **77**, 333–352.

White, T. E. 1939. Osteology of *Seymouria baylorensis* Broili. *Bulletin of the Museum of Comparative Zoölogy* **85(5)**, 323–409 + 3 pls.

Zouicha, A., Voigt, S., Saber, H., Marchetti, L., Hminna, A., El Attari, A., Ronchi, A. & Schneider, J. W. 2021. First record of permian continental trace fossils in the jebilet massif, Morocco. *Journal of African Earth Sciences* **173**, 104015. https://doi.org/10.1016/j.jafrearsci.2020.104015
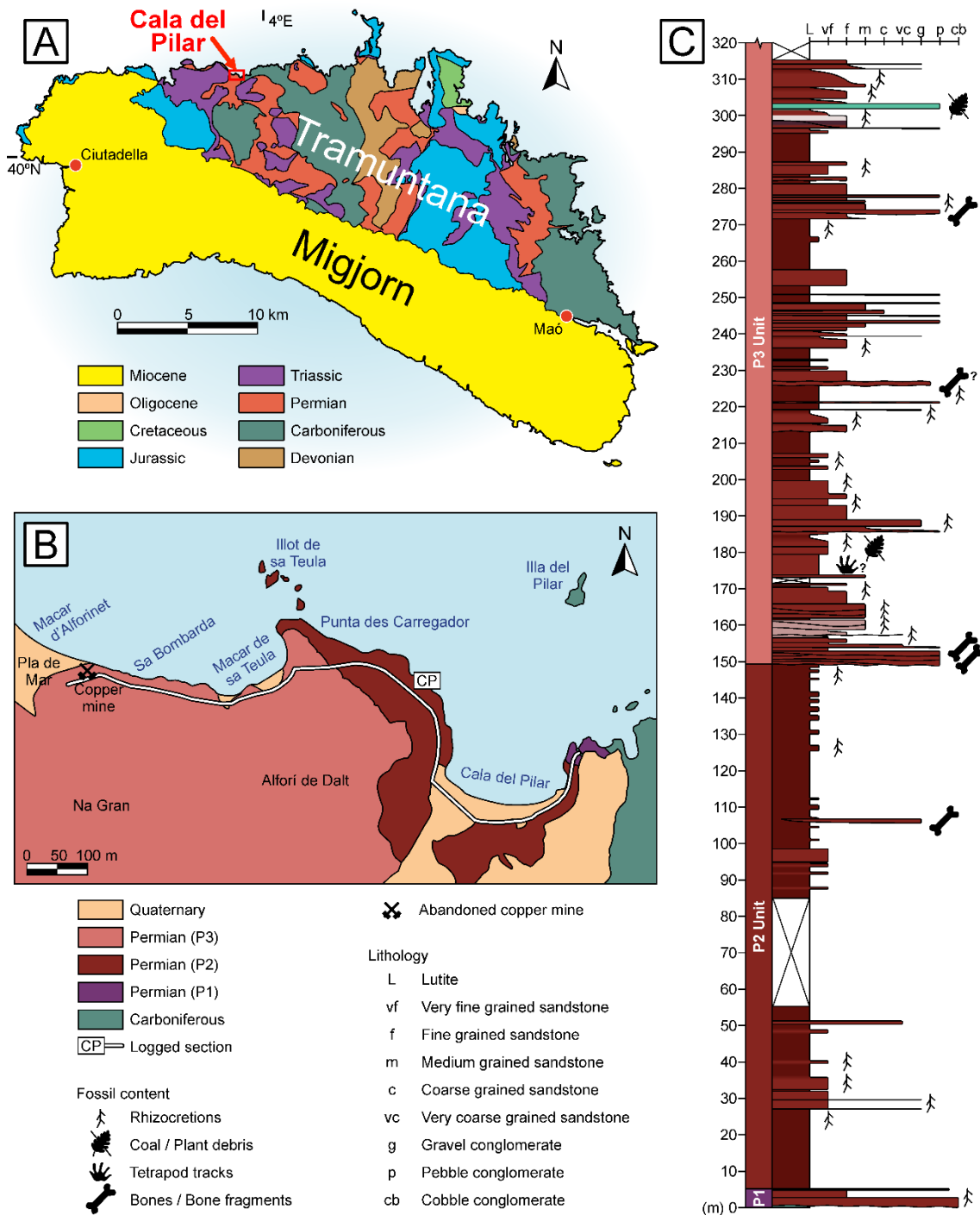
Figure 1. A: Geological map of Menorca (modified after Rosell *et al*. 1989a), indicating the location of Cala del Pilar. **B:** Detailed geological map of the study zone, indicating where the log was measured (toponyms after Buenaventura 2004). **C:** Synthetic stratigraphic log of Cala del Pilar–Pla de Mar section, indicating the fossiliferous horizons. Those with a question mark were found *ex situ* and attributed to that bed based on lithological equivalence.
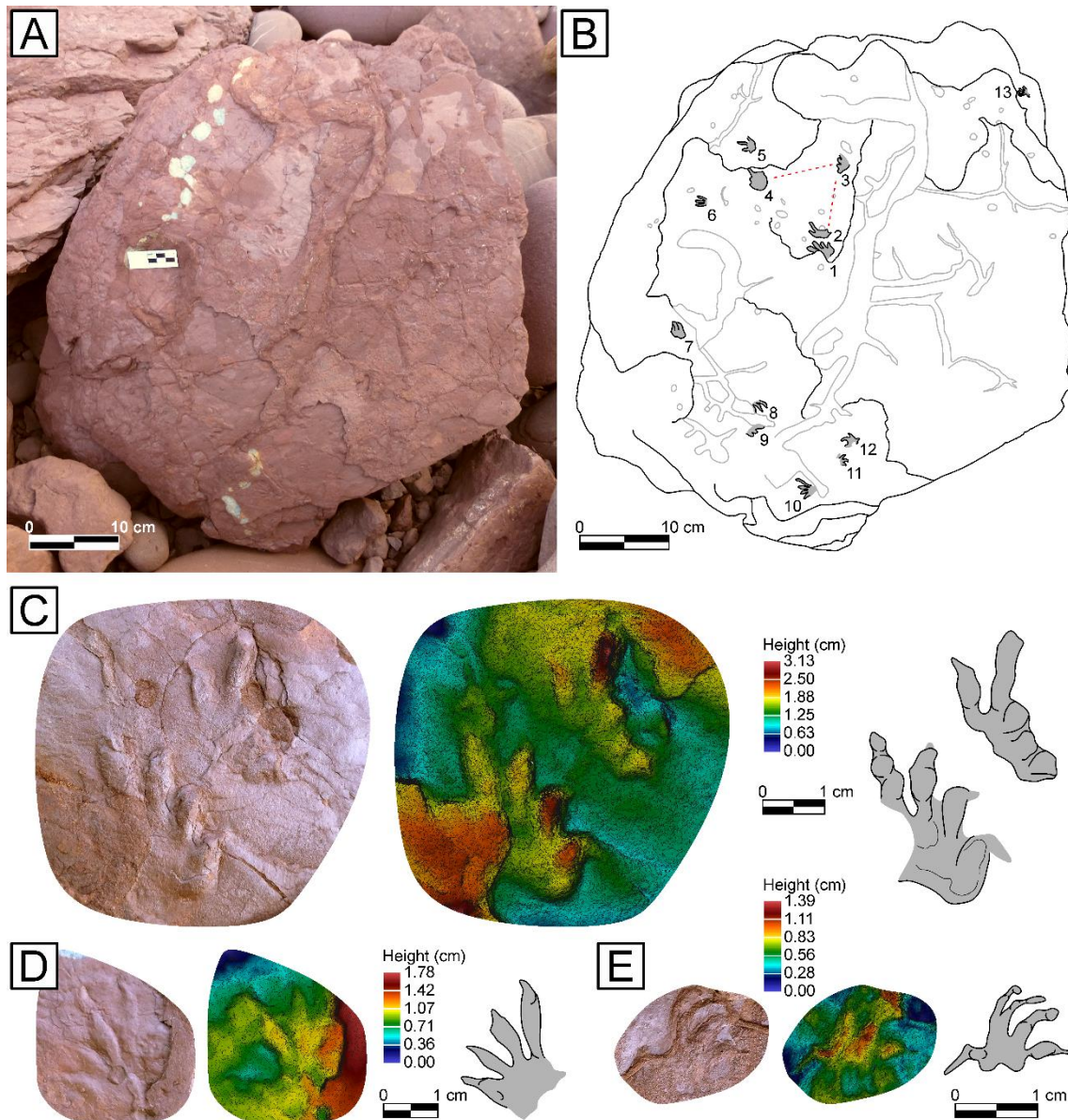
Figure 2. Ichnites of the boulder herein named MT01 from an indeterminate Permian of Cala del Pilar–Pla de Mar section (Menorca), with height models and interpretative drawings. **A:** Picture of MT01 as it was found. **B:** Interpretative drawing of MT01, with each number referring to a specific ichnite under the nomenclature MT01-[number]. **C:** Picture, false colour-coded height model and interpretative drawing of MT01-1 and MT01-2 (*Hyloidichnus* isp.). **D:** Picture, false colour-coded height model and interpretative drawing of MT01-10 (*Hyloidichnus* isp.). **E:** Picture, false colour-coded height model and interpretative drawing of MT01-13 (cf. *Erpetopus* isp.).
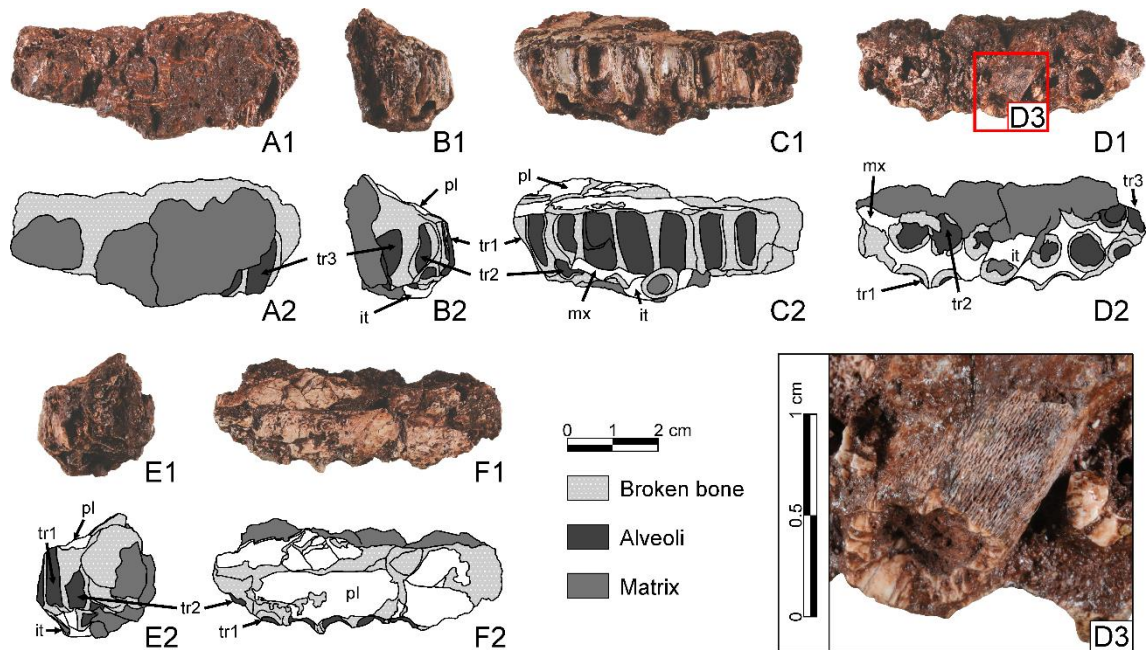
Figure 3. Holotype specimen of *Balearosaurus bombardensis* gen. et sp. nov. (IPS35597, right maxillar and palatine), from an indeterminate Permian of Cala del Pilar–Pla de Mar section (Menorca). **A:** labial view, **B:** anterior view, **C:** lingual view, **D:** occlusal view, **E:** posterior view, **F:** dorsal view. **it:** isolated tooth; **mx:** maxillar; **pl:** palatine; **tr1–3:** teeth row 1–3. All specimens in the same scale except for D3.
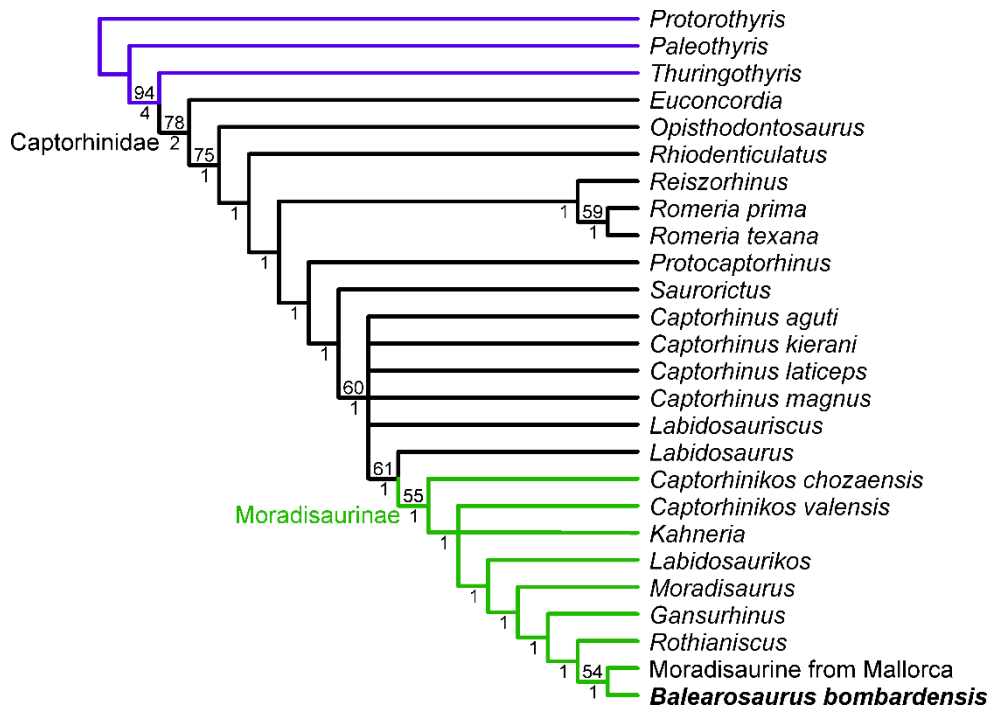
Figure 4. Strict consensus of the best 36 trees recovered (tree length = 251 steps) of the Captorhinomorpha, including the large moradisaurines of the Balearic Islands, using a branch-and-bound search. Consistency index (CI) = 0.553, retention index (RI) = 0.756. Double-digit numbers on the branches represent the bootstrap support values (n = 1000, values under 50 not shown), and single digits below represent the Bremer decay support value of that node.
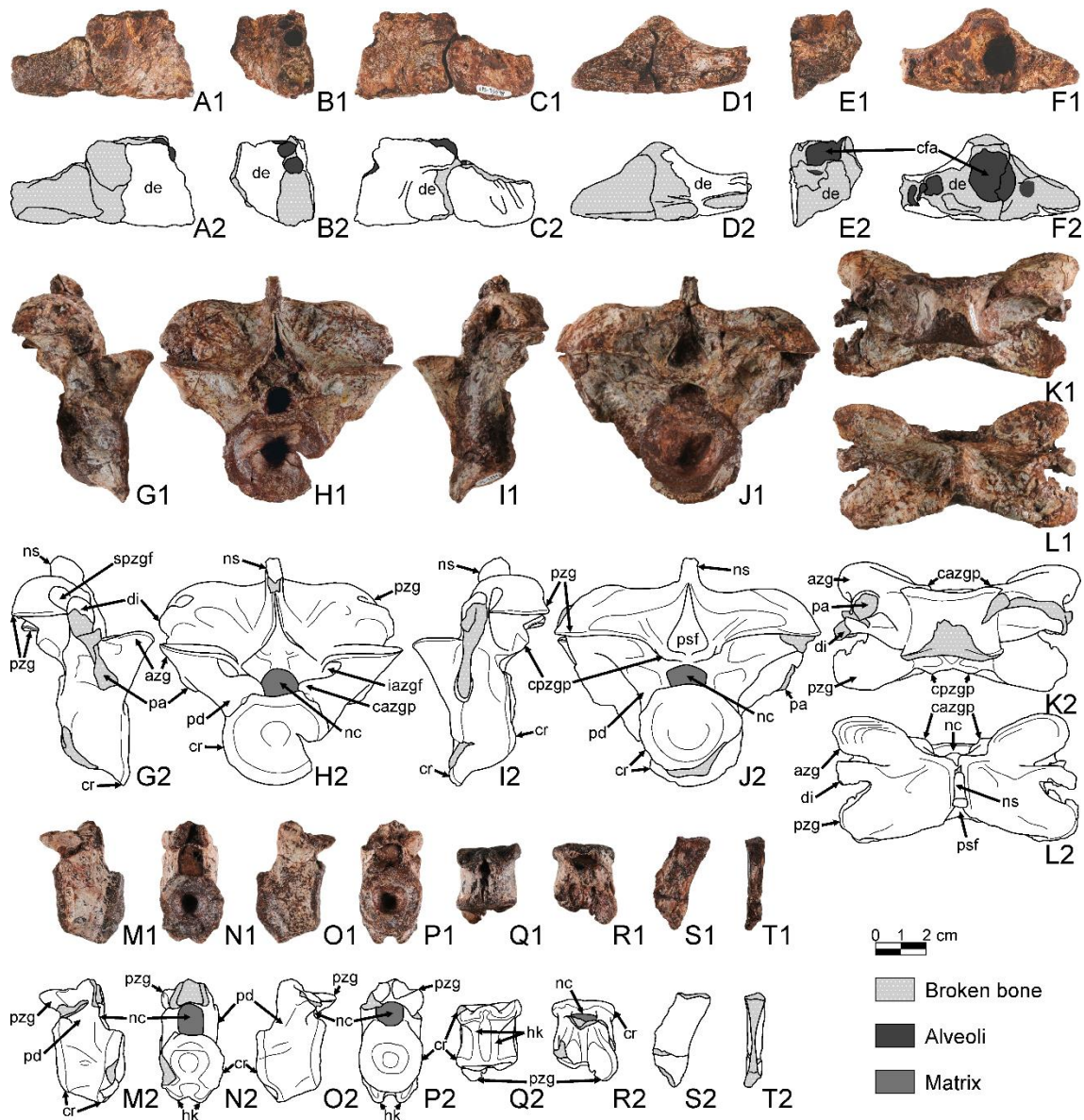
Figure 5. Pictures and interpretative drawings of cranial and axial elements of cf. *Balearosaurus bombardensis* gen. et sp. nov. from an indeterminate Permian of Cala del Pilar–Pla de Mar section (Menorca). **A–F:** IPS35598, distal fragment of left jaw. **A:** lingual view, **B:** anterior view, **C:** labial view, **D:** ventral view, **E:** posterior view, **F:** occlusal view. **G–L:** IPS35592, anterior dorsal vertebra. **G:** right lateral view, **H:** anterior view, **I:** left lateral view, **J:** posterior view, **K:** ventral view, **L:** dorsal view. **M–R:** IPS35590, middle caudal vertebra. **M:** right lateral view, **N:** anterior view, **O:** left lateral view, **P:** posterior view, **Q:** ventral view, **R:** dorsal view. **S–T:** IPS35588, possible fragment of haemal arch. **S:** right lateral view, **T:** anterior view. **azg:** prezygapophysis; **cazgp:** centroprezygapophyseal process; **cfa:** alveolus of caniniform; **cpzgp:** centropostzygapophyseal process; **cr:** cortical rim; **de:** dentary; **di:** diapophysis; **hk:** haemal keel; **iazgf:** infraprezygapophyseal fossa; **nc:** neural canal; **ns:** neural spine; **pa:** parapophysis; **pd:** pedicel; **pl:** palatine; **psf:** postspinal fossa; **pzg:** postzygapophysis; **spzgf:** suprapostzygapophyseal fossa.
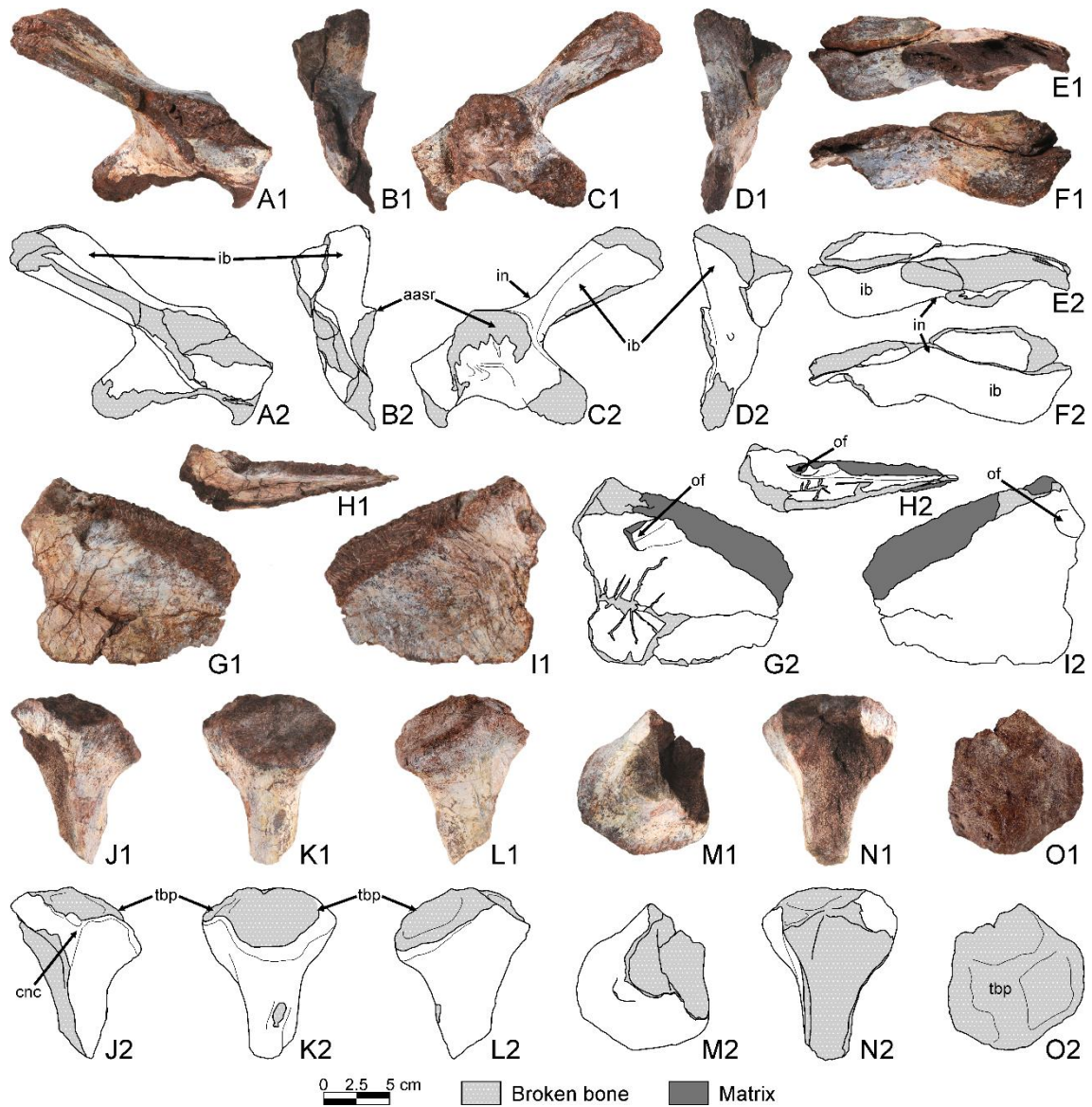
Figure 6. Pictures and interpretative drawings of girdle and limb elements of cf. *Balearosaurus bombardensis* gen. et sp. nov. from an indeterminate Permian of Cala del Pilar–Pla de Mar section (Menorca). **A–F:** IPS120163, right ilium. **A:** lateral view, **B:** anterior view, **C:** medial view, **D:** posterior view, **E:** ventral view, **F:** dorsal view. **G–I:** IPS120164, left pubis, **G:** medial view, **H:** ventral view, **I:** lateral view. **J–O:** IPS120165, fragment of the proximal epiphysis of a left tibia. **J:** extensor view, **K:** lateral view, **L:** flexor view, **M:** distal view, **N:** medial view, **O:** proximal view. **aasr:** area of attachment of sacral ribs; **cnc:** cnemial crest; **ib:** iliac blade; **in:** iliac neck; **of:** obturator foramen; **tbp:** tibial plateau.
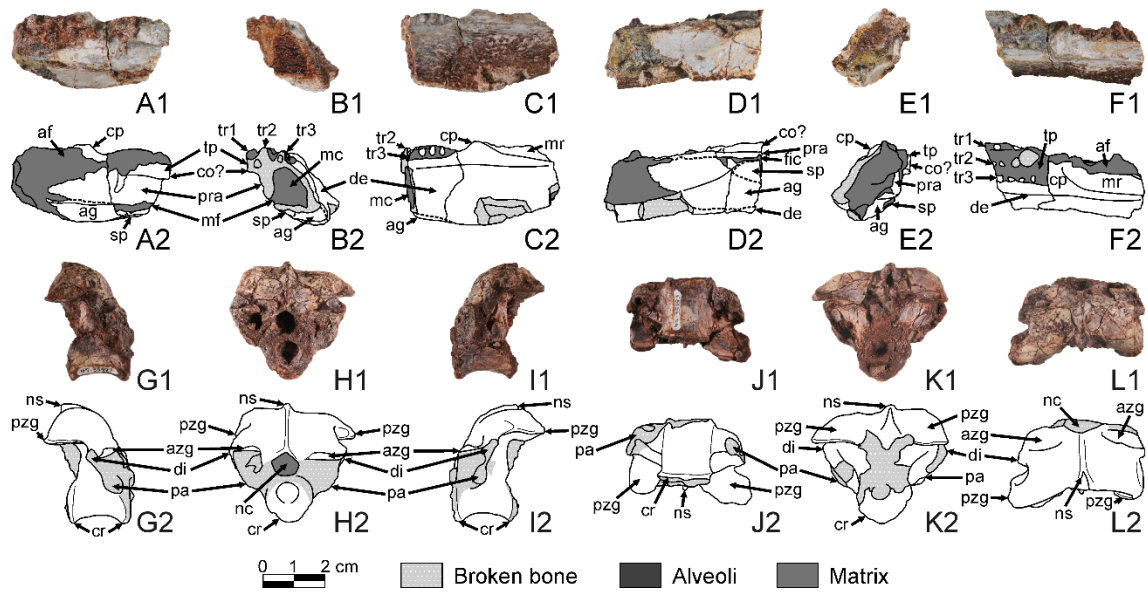
Figure 7. Pictures and interpretative drawings of cranial and axial elements of Moradisaurinae indet. from an indeterminate Permian of Cala del Pilar–Pla de Mar section (Menorca). **A–F:** IPS120166, proximal fragment of left jaw. **A:** lingual view, **B:** anterior view, **C:** labial view, **D:** ventral view, **E:** posterior view, **F:** occlusal view. **G–L:** IPS35588, middle/posterior dorsal vertebra. **G:** right lateral view, **H:** anterior view, **I:** left lateral view, **J:** posterior view, **K:** ventral view, **L:** dorsal view. **af:** adductor fossa; **ag:** angular; **azg:** prezygapophysis; **co:** coronoid; **cp:** coronoid process; **cr:** cortical rim; **de:** dentary; **di:** diapophysis; **mc:** mandibular canal; **mf:** Meckelian foramen; **mr:** mandibular ramus; **nc:** neural canal; **ns:** neural spine; **pa:** parapophysis; **pd:** pedicel; **pra:** prearticular; **pzg:** postzygapophysis; **sp:** splenial; **tp:** teeth plate; **tr1–3:** teeth row 1–3.
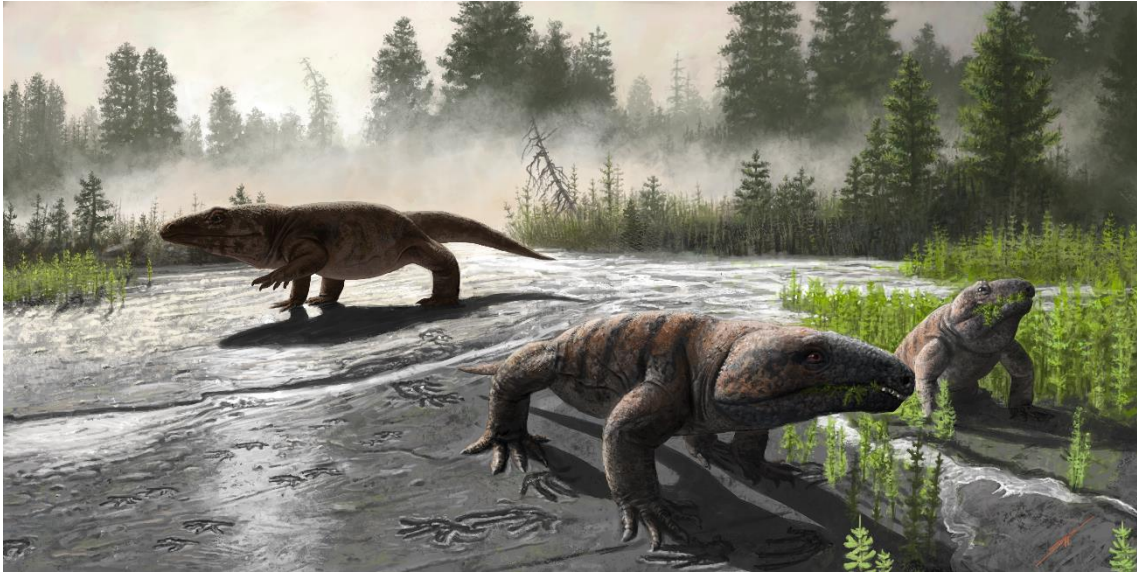
Figure 8. Reconstruction of the palaeoassemblage of the Permian P3 unit of Menorca, representing one specimen of *Balearosaurus bombardensis* gen. et sp. nov. (background) and two specimens of the smaller Moradisaurinae indet. (foreground), wandering on a crevasse splay lobe and leaving their tracks (*Hyloidichnus*) near other cf. *Erpetopus* tracks. Created by Henry Sutherland Sharpe. © 2021 Henry Sutherland Sharpe. Used under license.
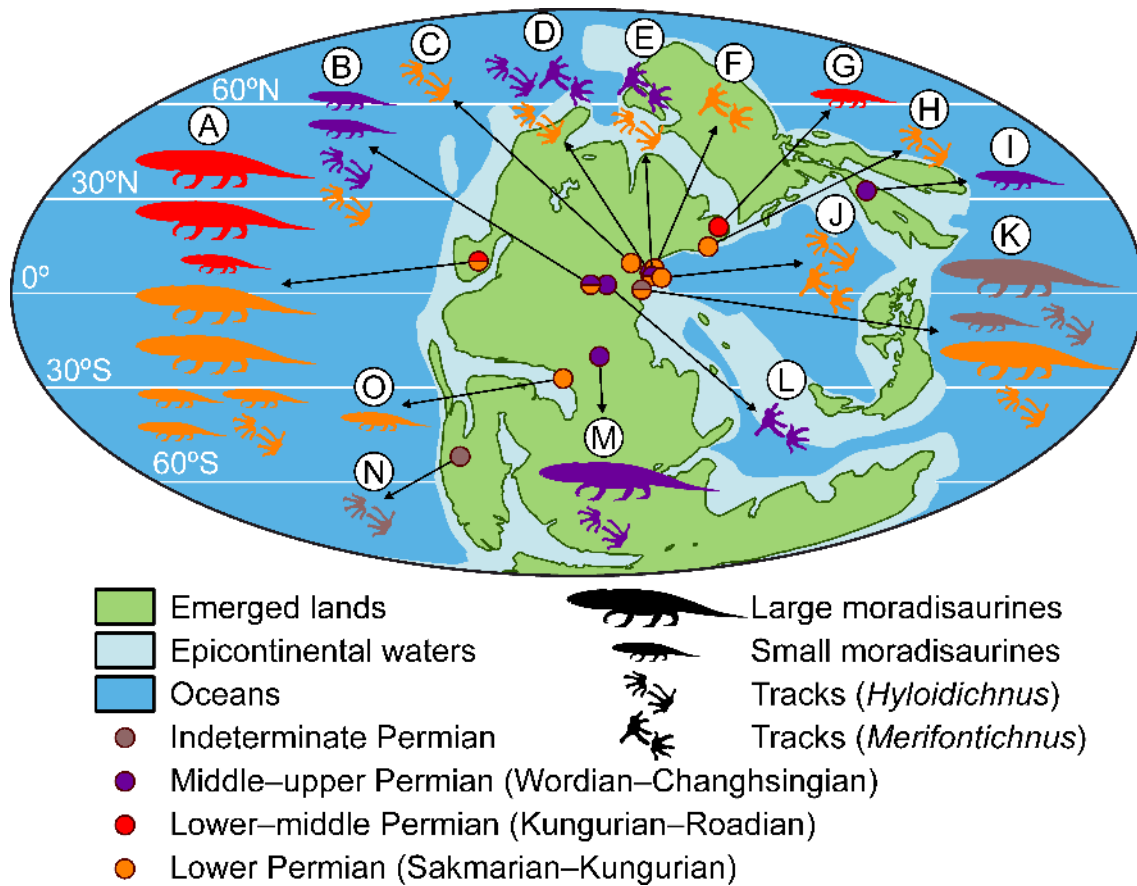
Figure 9. World map during the Permian (modified from Scotese 2014) with the localities that have yielded bones and tracks of possible moradisaurine captorhinid eureptiles. **A:** *Captorhinikos chozaensis*, *Captorhinikos parvus*, *Captorhinikos valensis*, *Labidosaurikos meachami*, a tooth plate from an indeterminate species and *Hyloidichnus* isp. from the lower Permian (Gilmore 1927; Stovall 1950; Olson 1954, 1962b, 1970; Haubold *et al.* 1995; Lucas *et al.* 2013; Modesto *et al.* 2014, 2016; LeBlanc *et al.* 2015; Voigt & Lucas 2015, 2017; Schneider *et al.* 2020), and *Kahneria seltina*, *Rothianiscus multidonta* and *Rothianiscus robusta* from the lower–middle Permian of southern North America (Olson & Beerbower 1953; Olson 1962a, 1965; Olson & Barghusen 1962). **B:** *Hyloidichnus* isp. from the lower Permian (Voigt *et al.* 2011; Zouicha *et al.* 2021), and *Acrodenta irerhi*, an indeterminate moradisaurine and *Hyloidichnus* isp. from the middle–upper Permian of northeastern Africa (Jalil & Dutuit 1996; Hmich *et al.* 2006; Voigt *et al.* 2010; Hminna *et al*. 2012; Moreau *et al.* 2020). **C:** *Hyloidichus* isp. from the lower Permian of northern Iberian Peninsula (Gand *et al*. 1997; López-Gómez *et al.* 2019b). **D:** *Hyloidichnus* isp. from the lower Permian, and *Hyloidichnus* isp. and *Merifontichnus* isp. from the middle Permian of southern Massif Central and Provence (Heyler & Lessertisseur 1963; Gand 1988, 1993; Gand *et al.* 2000; Gand & Durand 2006; Michel *et al.* 2015; Logghe *et al.* 2021). **E:** *Hyloidichnus* isp. from the lower Permian (Voigt & Haubold 2015; Mujal *et al.* 2016) and possible *Merifontichnus* isp. from the middle Permian of the Pyrenees (Mujal *et al.* 2017). **F:** *Merifontichnus* isp. from the lower Permian of Sardinia (Citton *et al.* 2019; Santi *et al.* 2020). **G:** *Gecatogomphius kavejevi* from the

middle Permian of eastern Europe (Vjushkov & Chudinov 1957; Olson 1962a; Ivakhnenko 2008). **H:** *Hyloidichnus* isp. from the lower Permian of northern Anatolia (Gand *et al*. 2011). **I:** *Gansurhinus qingtoushanensis* from the middle–upper Permian of central-east Asia (Reisz *et al.* 2011). **J:** *Hyloidichnus* isp. and *Merifontichnus* isp. from the lower Permian of the Alps (Marchetti *et al*. 2013, 2015a, 2015b, 2015c; Marchetti 2016; Santi *et al.* 2020). **K:** indeterminate moradisaurine and *Hyloidichus* isp. from the lower Permian of Mallorca (Calafat *et al.* 1986, 1987; Calafat 1988; Gand *et al.* 2010; Liebrecht *et al.* 2017; Matamales-Andreu *et al.* 2019), and *Balearosaurus bombardensis* gen. et sp. nov., an indeterminate moradisaurine and *Hyloidichnus* isp. from an indeterminate Permian of Menorca (the present work). **L:** possible *Merifontichnus* isp. from the middle–upper Permian of north-central Africa (Contessi *et al.* 2018). **M:** *Hyloidichnus* isp. and *Moradisaurus grandis* from the middle–upper? Permian of central Africa (Ricqlès & Taquet 1982; O'Keefe *et al.* 2005; Smith *et al.* 2015; Olroyd & Sidor 2017; Modesto *et al.* 2019). **N:** *Hyloidichnus* isp. from an indeterminate Permian of southern South America (Melchor & Sarjeant 2004; Marchetti *et al.* 2020a). **O:** *Captorhinikos* sp. from the lower Permian of northern South America (Cisneros *et al.* 2020a).

Table 1. Set of measurements taken on selected footprints of MT01. Although all the ichnites have been numbered, only the best preserved ones have been measured. Columns without data correspond to poorly-preserved ichnites that have been used for trackway measurements, such as MT01-3, or to well-preserved ichnites without trackway information, such as MT01-10 and MT01-13.

Track parameters						
Footprint number	MT01-1 (right pes)	MT01-2 (right manus)	MT01-3 (left pes)	MT01-4 (right pes)	MT01-10 (left ?pes)	MT01-13 (right ?manus)
Identification	*Hyloidichnus* isp.					cf. *Erpetopus* isp.
Length (mm)	26.4	-	-	-	22.8	10.9
Width (mm)	-	-	-	-	-	11.5
Length sole (mm)	13.0	9.0	-	13.9	9.5	4.7
Width sole (mm)	-	15.0	-	12.6	12.5	5.5
Length I (mm)	6.7	-	-	-	7.3	4.3
Length II (mm)	10.0	-	-	-	8.8	6.4
Length III (mm)	11.4	-	-	-	11.3	7.6
Length IV (mm)	15.0	12.8	-	-	15.0	7.8
Length V (mm)	-	7.8	-	-	-	2.9
Divergence angle I–II (°)	15.4	-	-	-	16.7	44.3
Divergence angle II–III (°)	4.3	-	-	-	27.9	21.6
Divergence angle III–IV (°)	21.7	-	-	-	18.7	-
Divergence angle IV–V (°)	-	21.4	-	-	-	95.3
Divergence angle I–V (°)	-	-	-	-	-	161.5
Trackway parameters (in brackets, footprints taken into consideration for that measurement)						
Footprint numbers of each trackway	MT01-1, MT01-2, MT01-3, MT01-4 (right manus-pes set, left pes and right pes)				MT01-10 (left ?pes)	MT01-13 (right ?pes)
Pace angulation pes (°)	71.9 (1–3–4)				-	-
Pace angulation manus (°)	-				-	-
Divarication pes midline (°)	5.0 (1)				-	-
Divarication manus midline (°)	44.6 (2)				-	-
Stride pes (mm)	78.7 (1–4)				-	-
Stride manus (mm)	-				-	-
Pace pes (mm)	67.0 (mean of 1–3: 69.4, 3–4: 64.6)				-	-
Pace manus (mm)	-				-	-
Length pace pes (mm)	39.4 (mean of 1–3: 43.3, 3–4: 35.4)				-	-
Length pace manus (mm)	-				-	-
Width pace pes (mm)	54.0 (mean of 1–3: 54.0, 3–4: 54.0)				-	-
Width pace manus (mm)	-				-	-
Interpes distance (mm)	39.9 (1–3)				-	-
Intermanus distance (mm)	-				-	-
Manus-pes distance (mm)	12.9 (1–2)				-	-
Width external (mm)	-				-	-
Width internal (mm)	-				-	-
Glenoacetabular distance (mm)	-				-	-